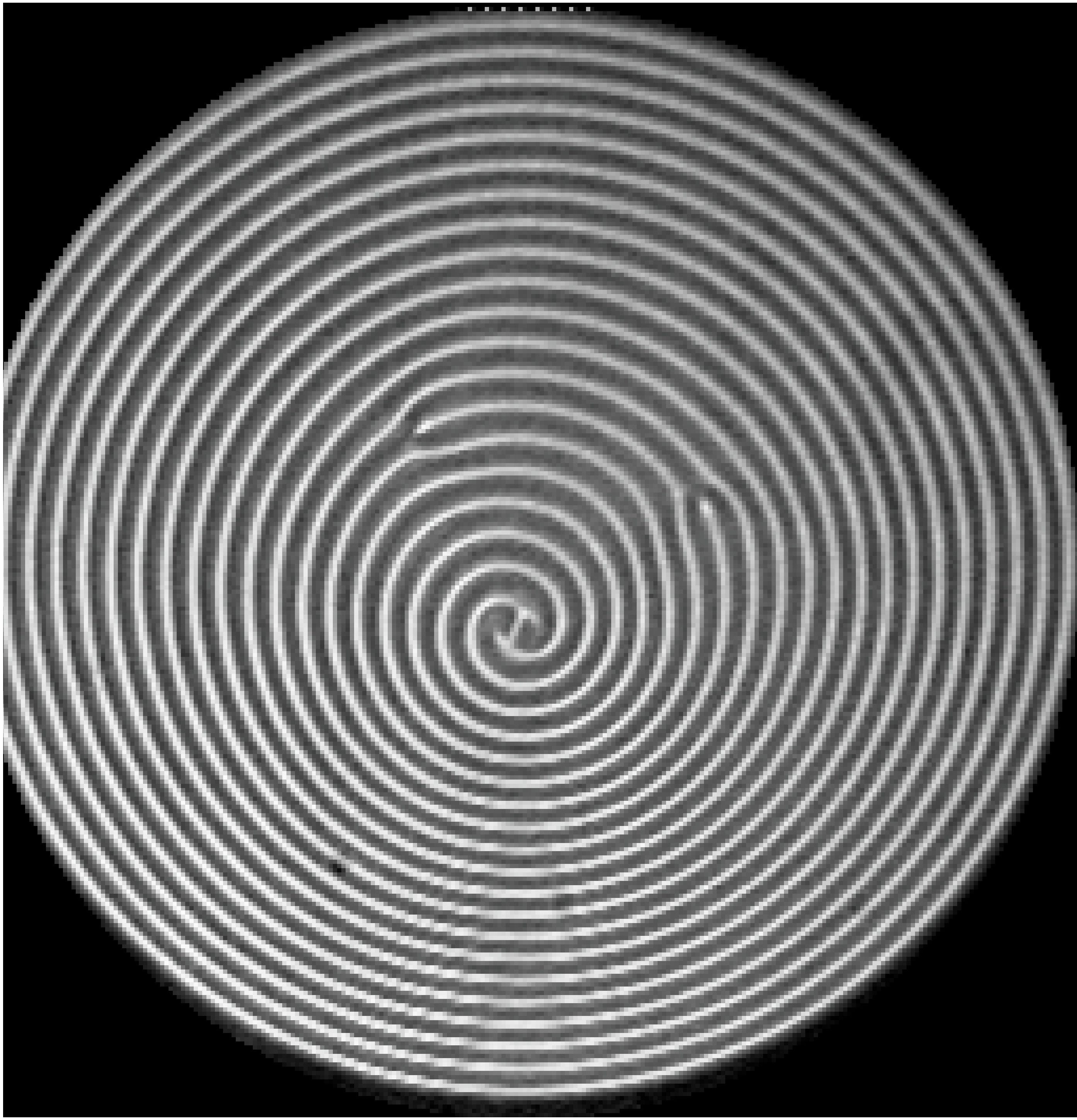

Oliver Brausch
Thomas Walter
Werner Pesch
Theoretische Physik II
University of Bayreuth

E.B.
Brendan B. Plapp
David Eolf
LASSP
Cornell University

NSF-DMR

Control Parameter:

$$\Delta T = T_{hot} - T_{cold}$$

Reduced Control Parameter:

$$\varepsilon = \frac{\Delta T - \Delta T_c}{\Delta T_c}$$

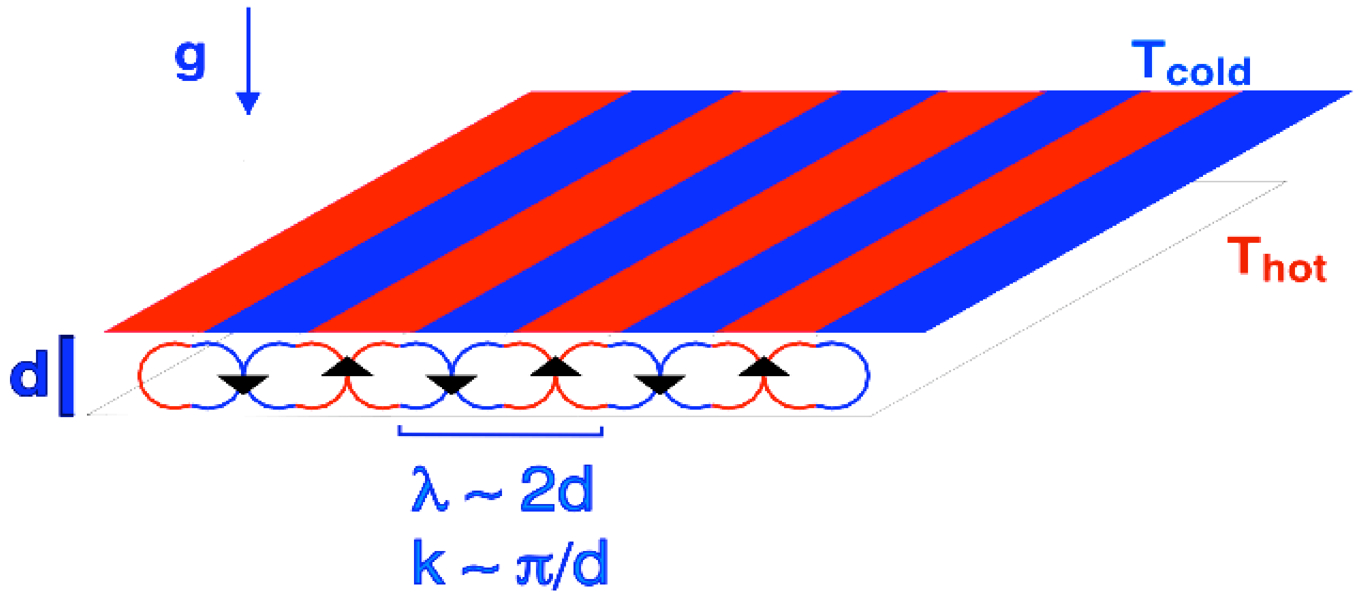

The stripes of warm upflow (red) and cold downflow (blue) constitute the pattern under consideration

Busse Balloon

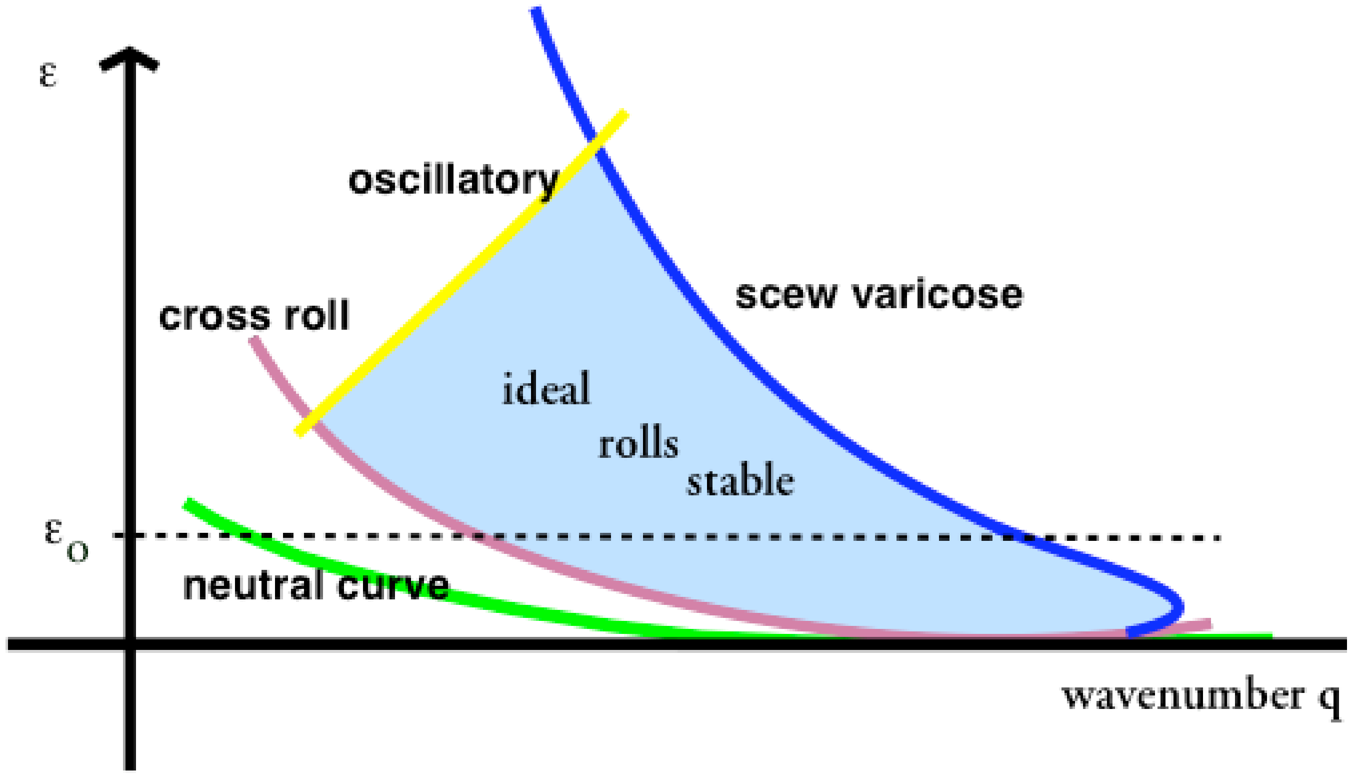

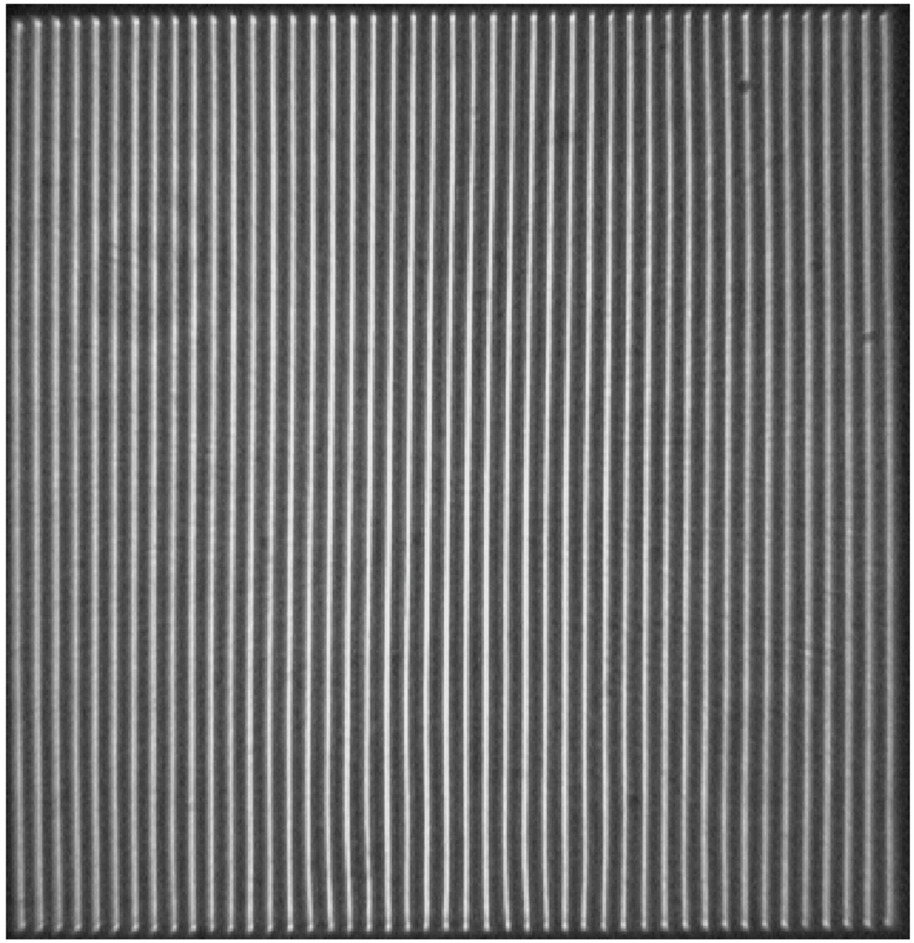

ideal rolls

pressure vessel with convection cell

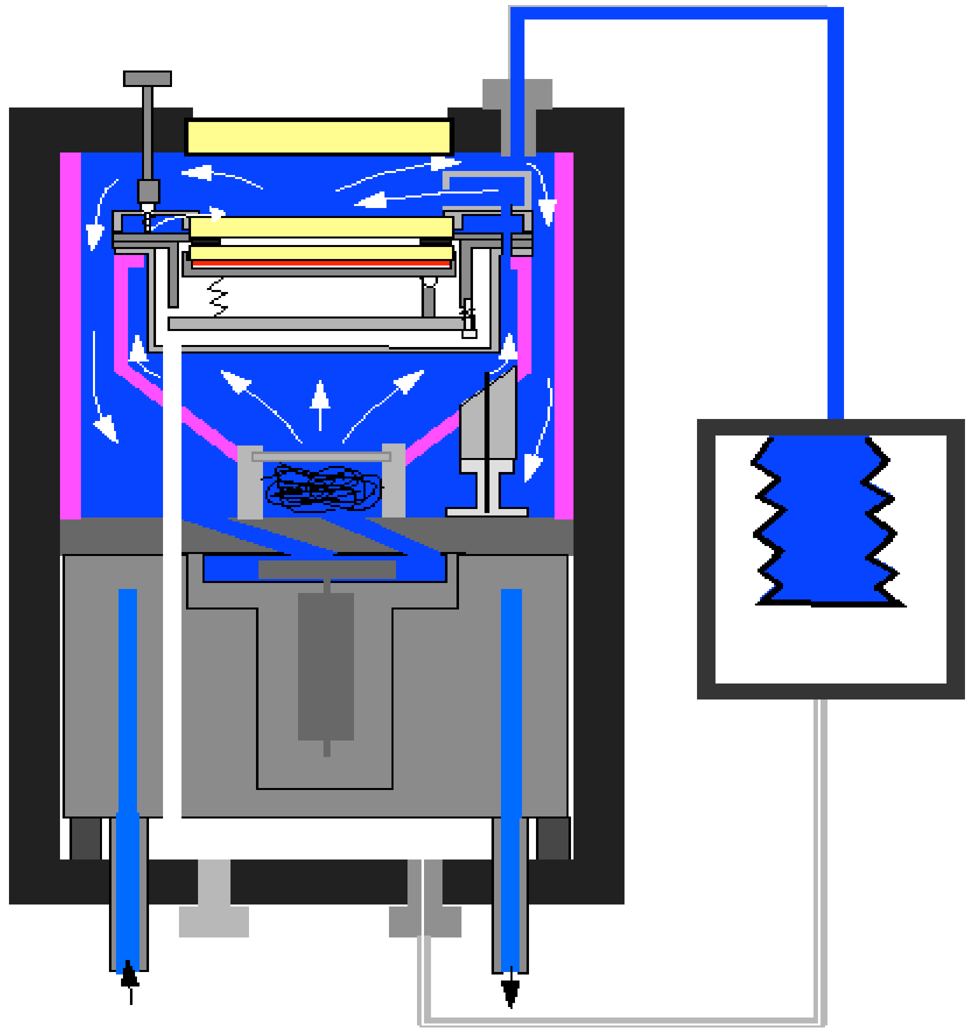

Rev. Sci. Instrum. 67 (1996) 2043

Shadowgraph Visualization

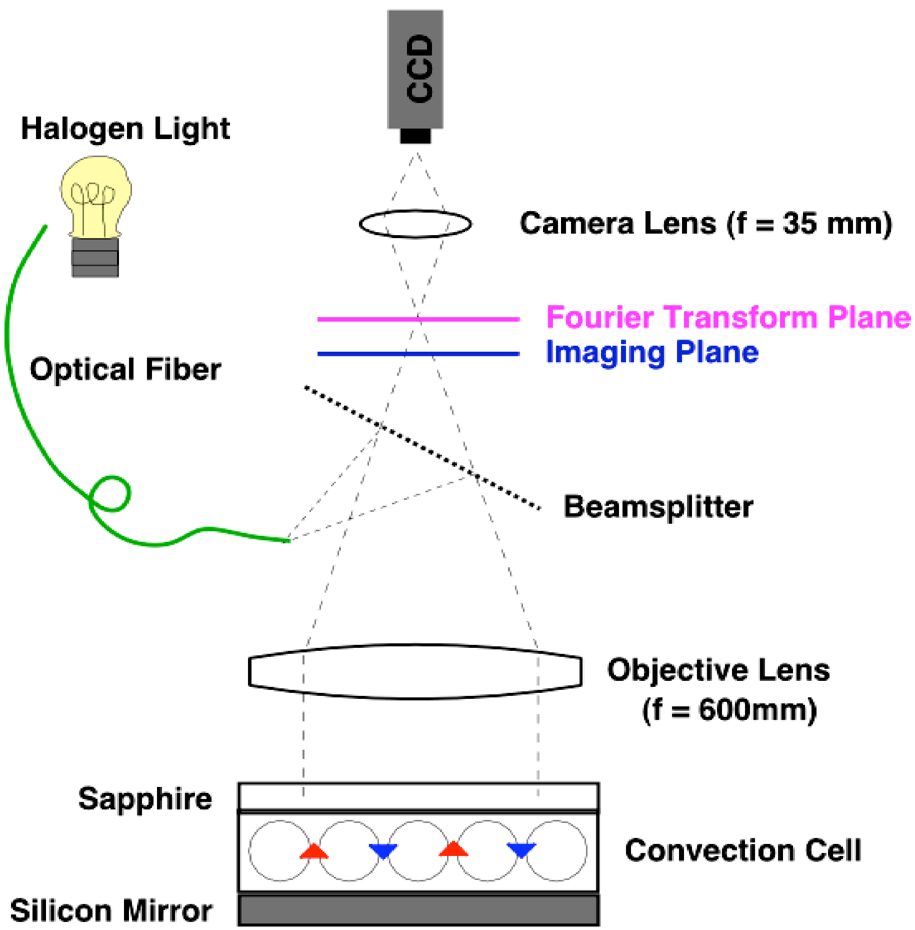

CO_2 gas pressurized to ~50 bar

top and bottom regulated to $\pm$ 0.2mK

plate separation 447μm, flatness ±0.5μm

thermal vert. diffusion time scale $d^2/\kappa \approx$ 2sec
viscous relaxation time scale $d^2/\nu \approx$ 1.5sec

Prandtl# $\nu/\kappa \approx$ 1.4sec

Boussinesq fluid $Q \approx -0.7$

Spiral Dynamics

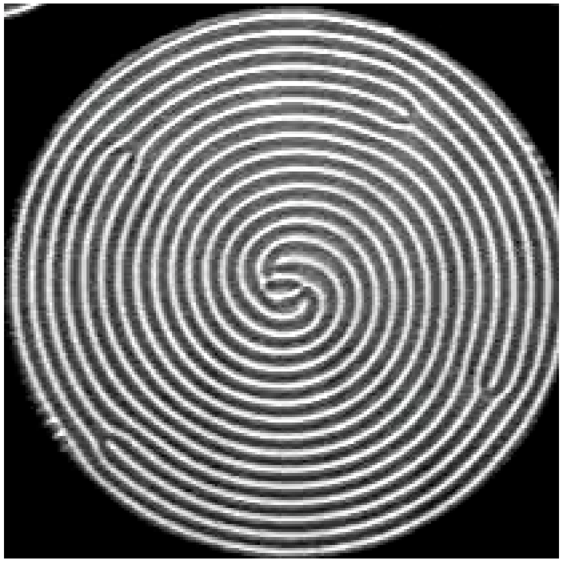

experiment

numerical simulation

Spiral Dynamics

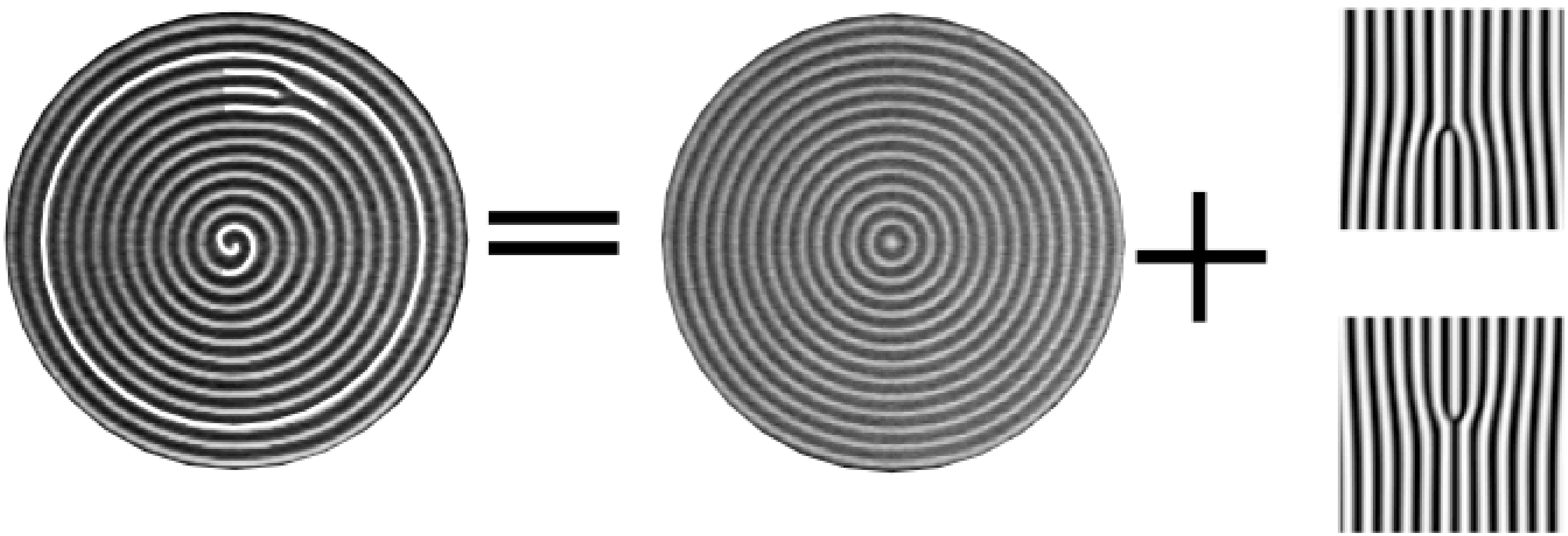

B. B. Plapp, D. A. Egolf, E. Bodenschatz, and W. Pesch
PRL 81, 5334 (1998)

TARGETS

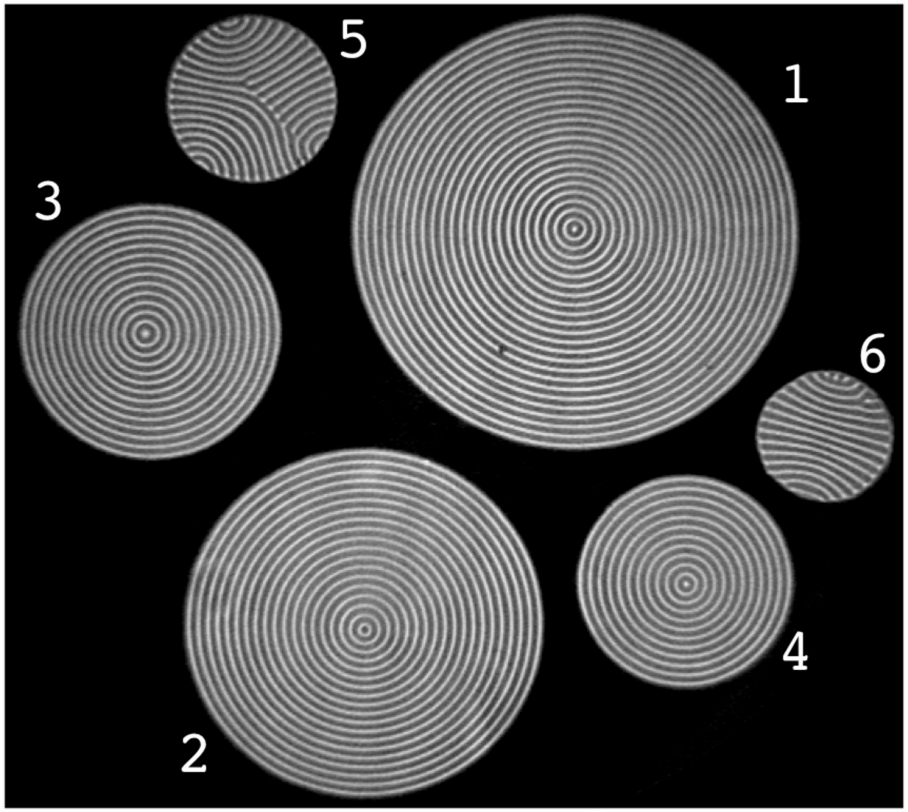

Figure 4.3: The six cylindrical convection cells at $\epsilon = 0.36$, $Pr = 1.39$. The cells are numbered in order of decreasing size.

Table 4.1: Lateral dimensions of cylindrical cell boundaries. Aspect ratio is the radial aspect ratio (radius/cell height, where the cell height is 447μm.)

Cell #	Radius (mm)	Aspect ratio	Step width min–max (mm)
1	21.6	48.4	0.9–1.2
2	17.3	38.8	0.4–0.5
3	12.7	28.4	0.6–1.1
4	10.6	23.8	0.5–0.8
5	8.5	19.1	0.0–0.8
6	6.7	14.9	0.0–0.4

What do we know about on-center targets?

- unstable above a certain driving - go off center
- spirals select a wavenumber q_T
- rolls travel to adjust wavenumber (inward - outward)

Nonlinear Phase Diffusion Equation

Cross, Newell, Passot, Tu …..

$$\boxed{\frac{\partial \Phi}{\partial T} + \rho(q)\mathbf{U} \cdot \nabla\Phi + \frac{1}{\tau(q)}\nabla \cdot [\mathbf{q}B(q)]}$$

perturbation around ideal rolls:

$$\boxed{\partial_t \phi = D_{||}\partial_x^2\phi + D_\perp \partial_y^2 \phi}$$

Phase diffusion coefficients

$$\boxed{\begin{aligned} D_{||}(q) &= -\frac{1}{\tau(q)}\frac{d}{dq}[qB(q)] \\ D_{\perp}(q) &= -\frac{1}{\tau(q)}B(q) \end{aligned}}$$

target selects: $D_{\perp} = 0$ ==> q_T

Eckhaus instability: $\left.\dfrac{\sigma(q)}{K^2}\right|_{K\to 0} = -D_{||}(q).$

wavenumber adjustment: $$\omega = -2\frac{q_T B'(q_T)}{\tau(q_T)}\frac{\Delta q(r)}{r}$$

with
$$\begin{aligned} D_{\|}(q_T) &= -\frac{1}{\tau(q_T)}\frac{d}{dq}[qB(q)]_{q_T} \\ &= -\frac{1}{\tau(q_T)}\left[q_T B'(q_T) + B(q_T)\right] \end{aligned}$$

$$\boxed{\omega = 2D_{\|}(q_T)\frac{\Delta q(r)}{r}}$$

$$\omega = 2D_{||}(q_T)\frac{\Delta q(r)}{r}$$

Velocity of traveling wave:

$$\boxed{v_R \simeq \frac{\alpha(q_T - q)}{qR_D}}$$

$$\alpha = 2D_{||}(q_T) = -2\left.\frac{\sigma(q_T)}{K^2}\right|_{K\to 0}$$

Target Instability

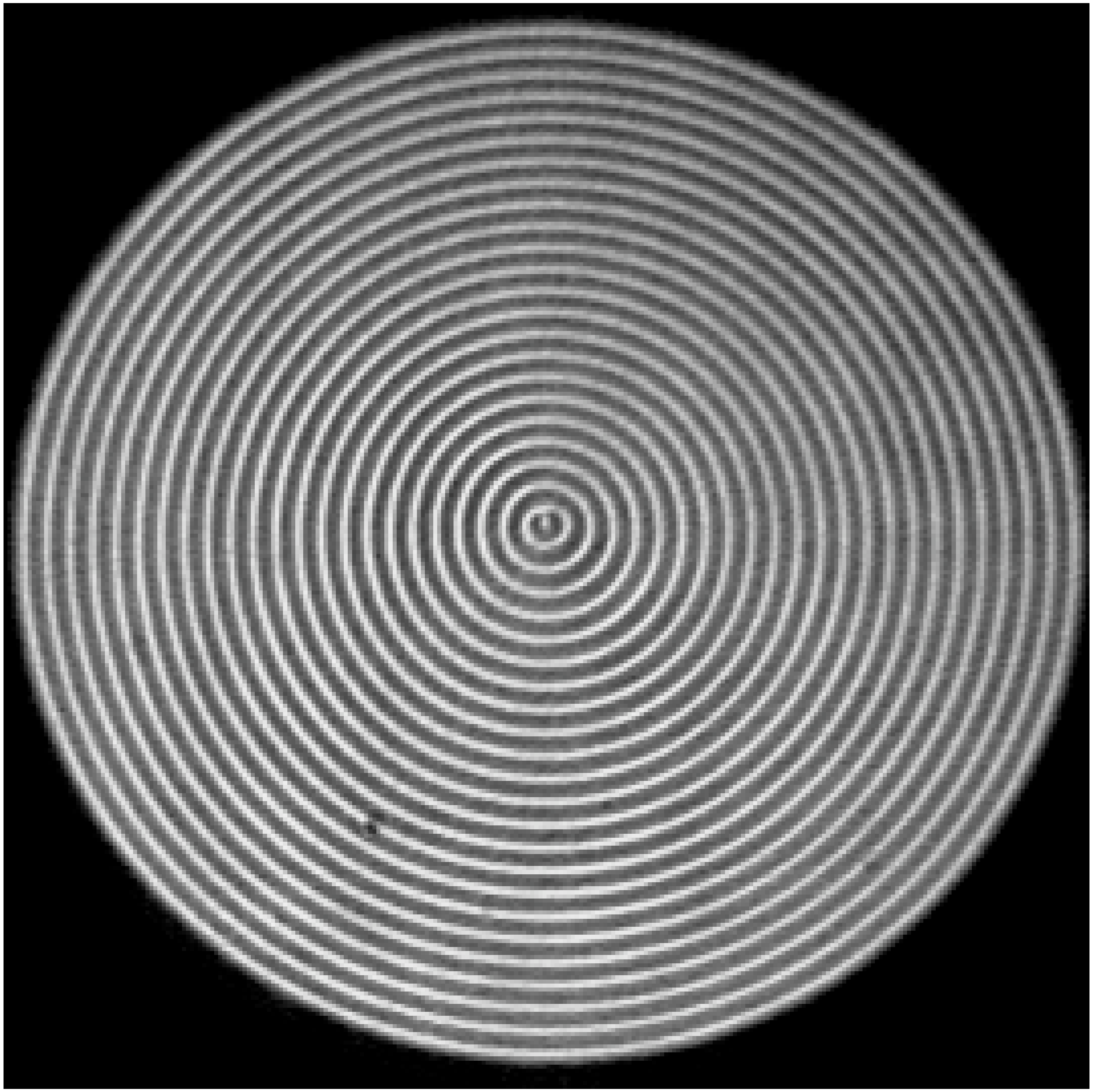
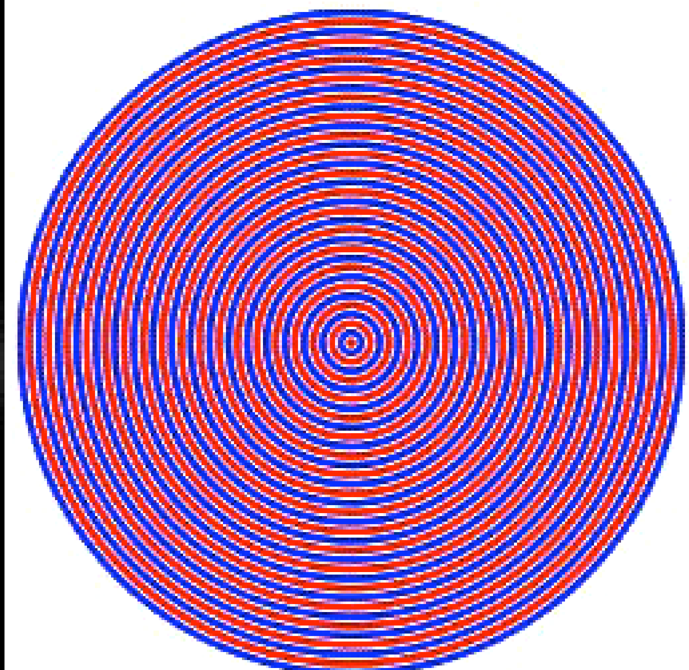

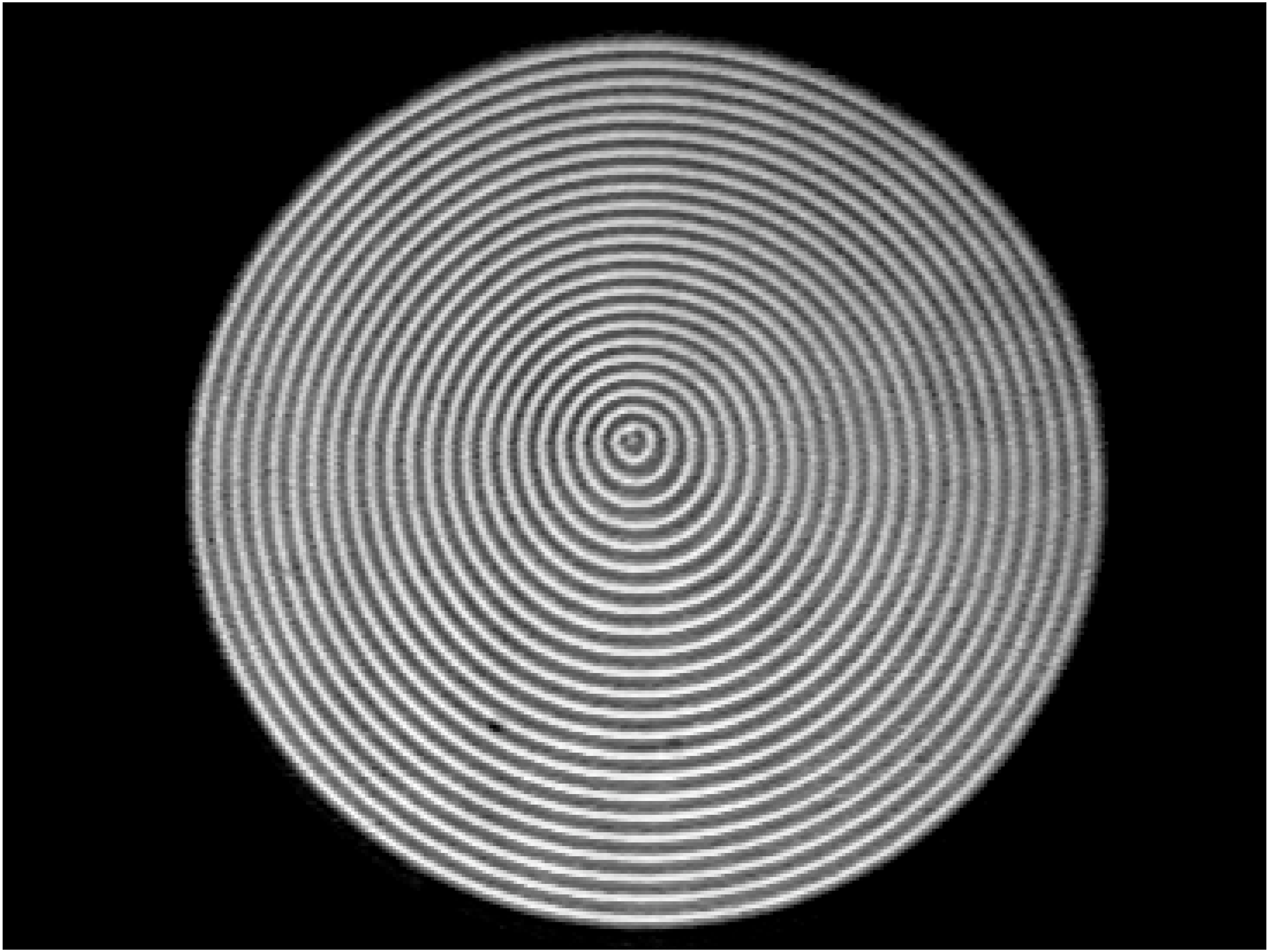

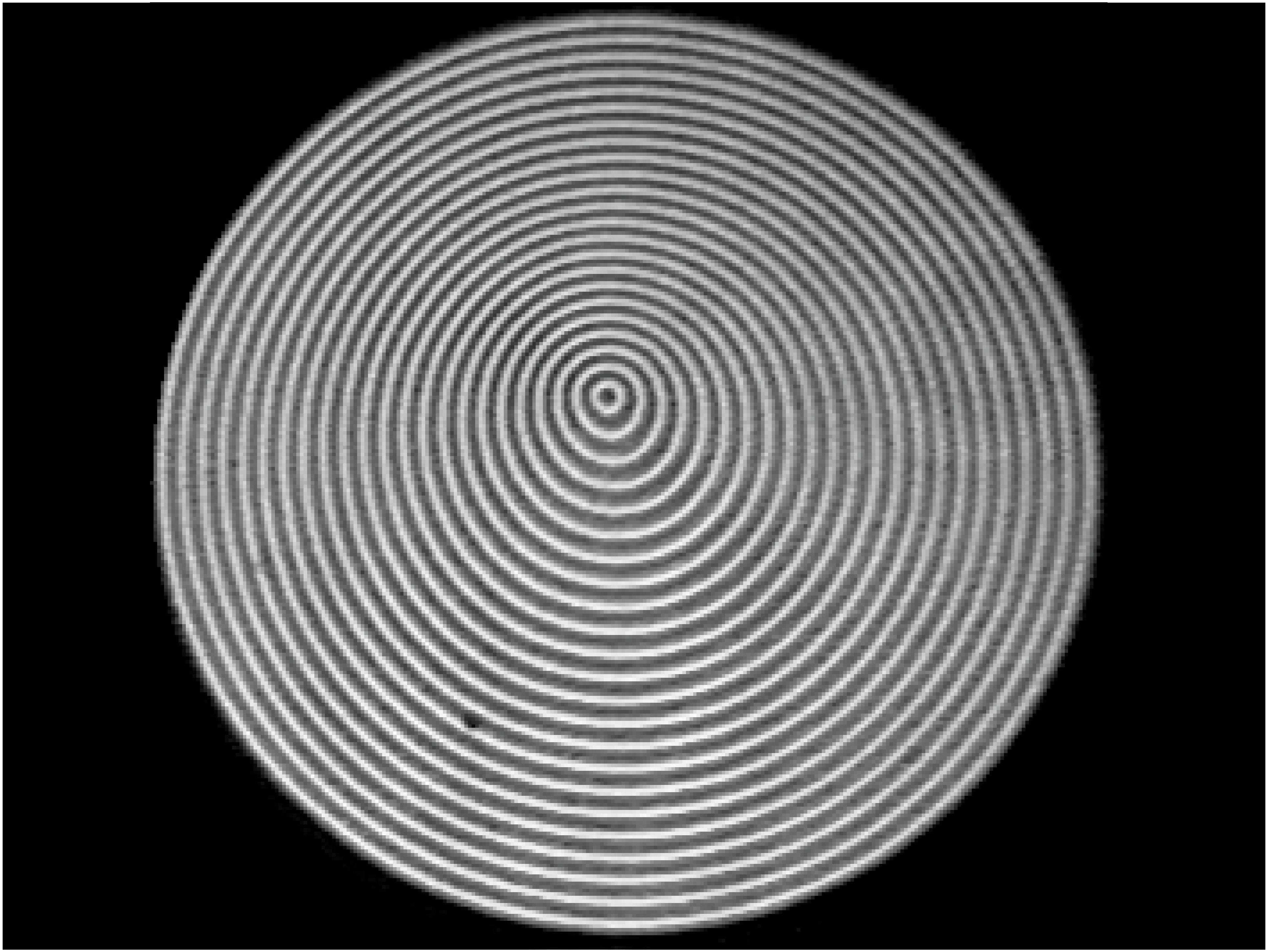

Target Instability

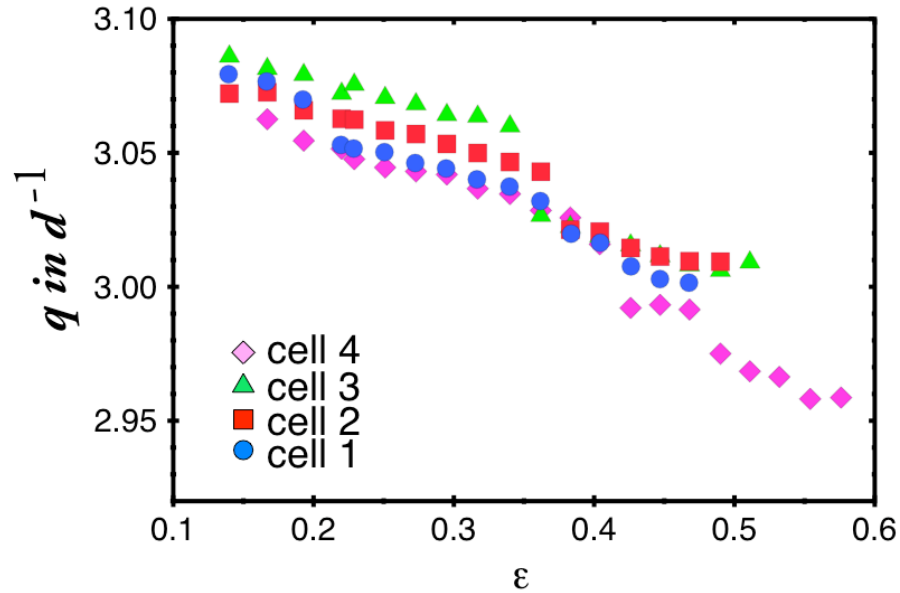

fit to cells 1, 2, and 3 gives:

$$q_t = 3.116 - 0.23 \ \varepsilon$$

numerical results (*Buell and Catton, Phys. Fluids* **29** *(1986) 23)*

$$q_t = 3.116 - 0.20 \ \varepsilon \ \checkmark$$

Spiral Dynamics

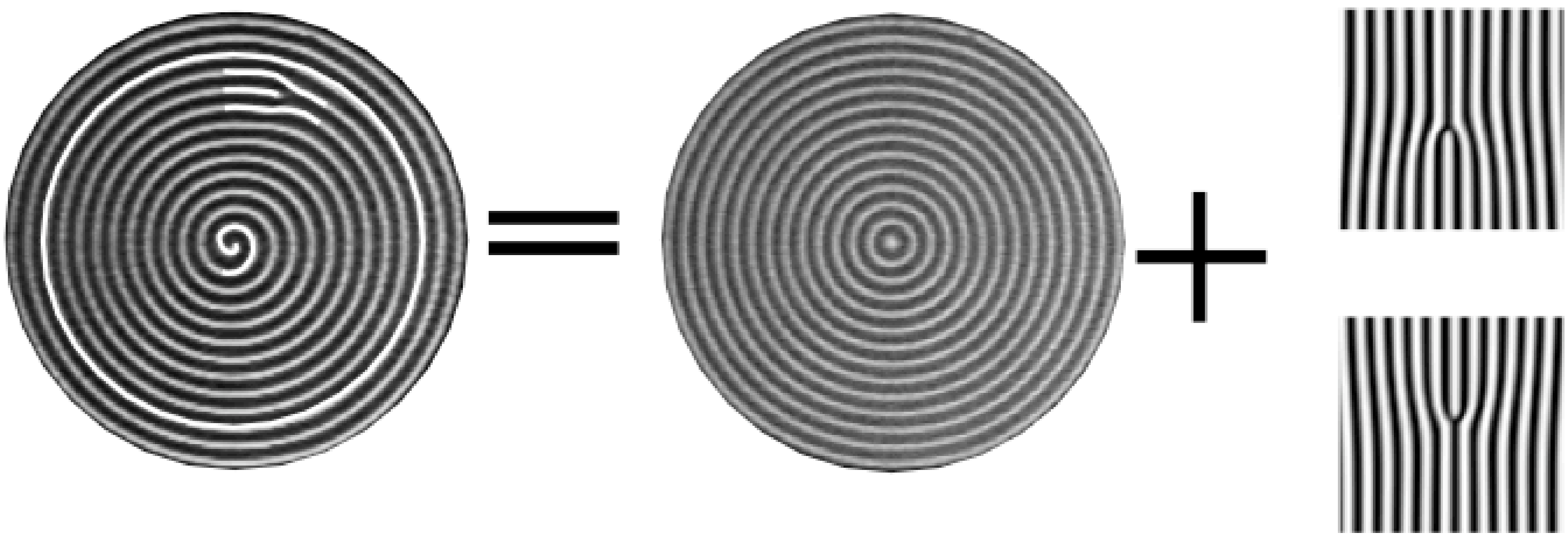

B. B. Plapp, D. A. Egolf, E. Bodenschatz, and W. Pesch
PRL 81, 5334 (1998)

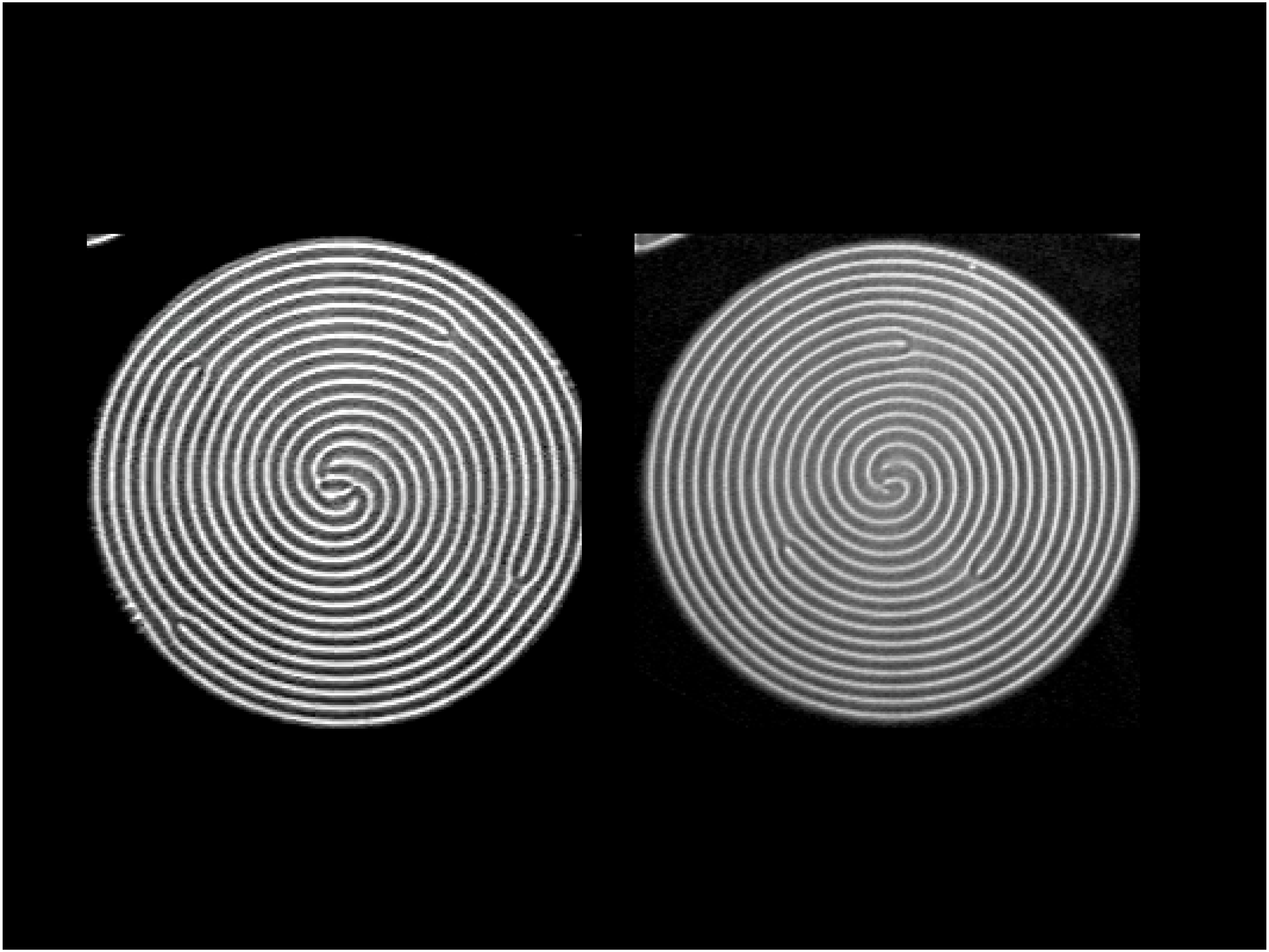

Averaging over one period

one-armed spiral

picture | *average*

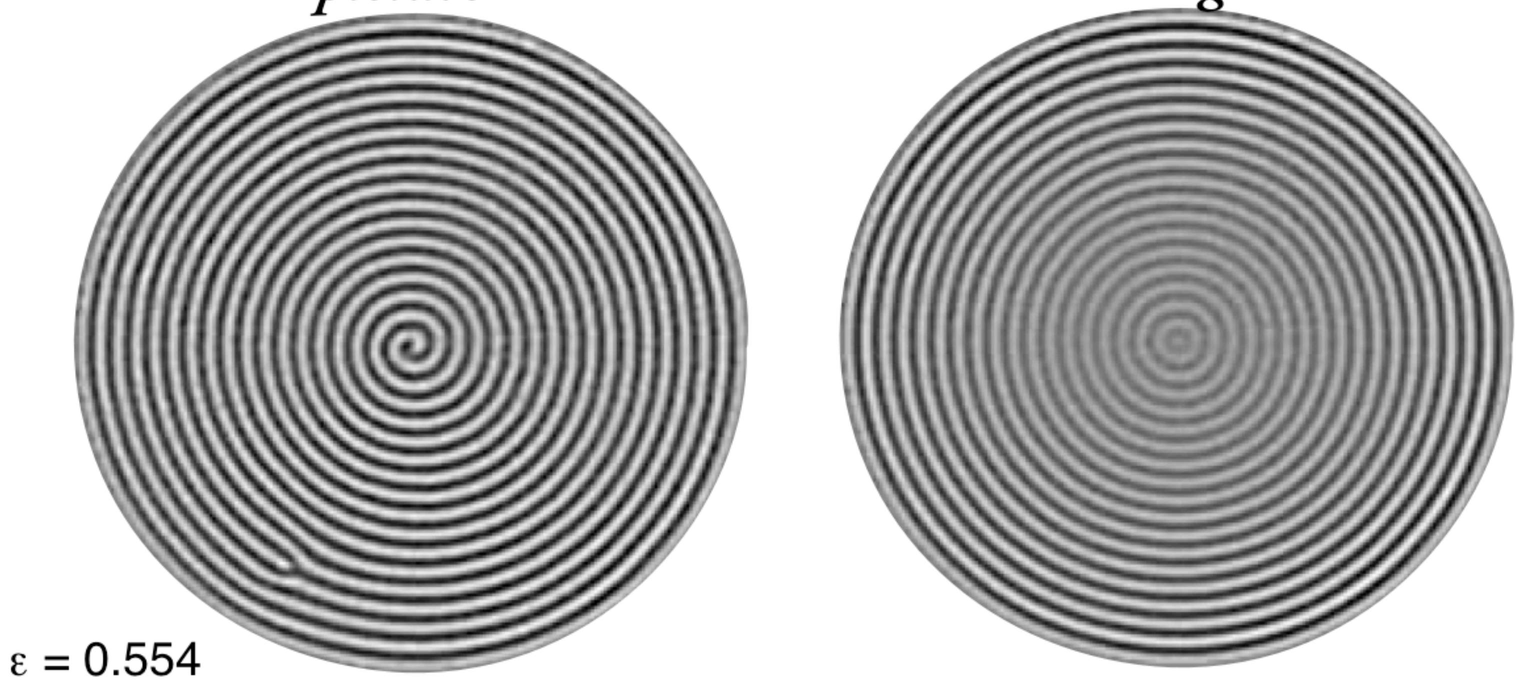

average gives target !

four-armed spiral

picture

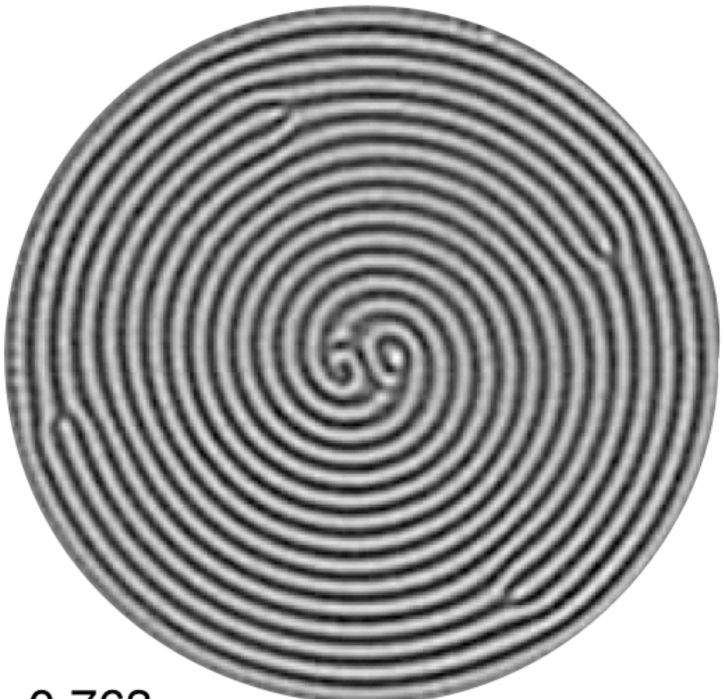

$\varepsilon = 0.763$

average

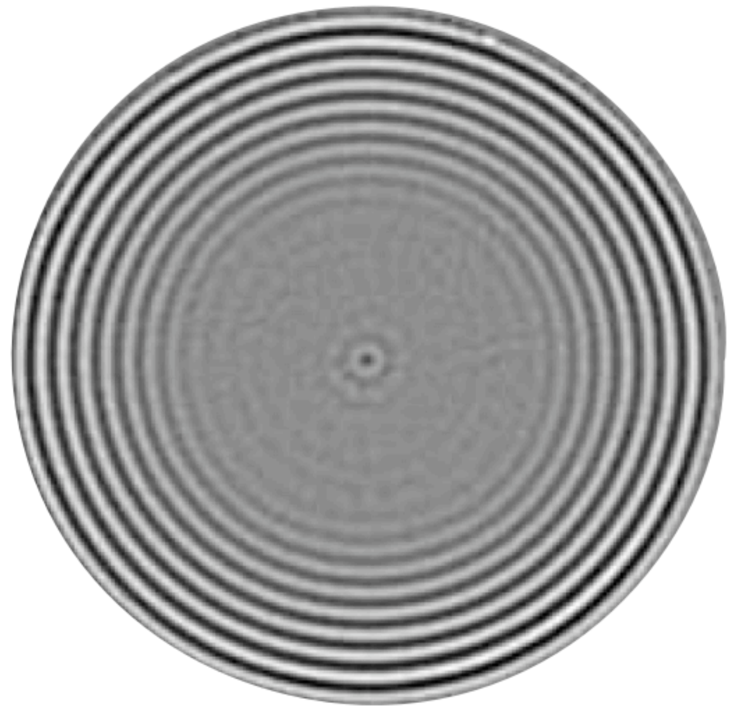

average gives target !

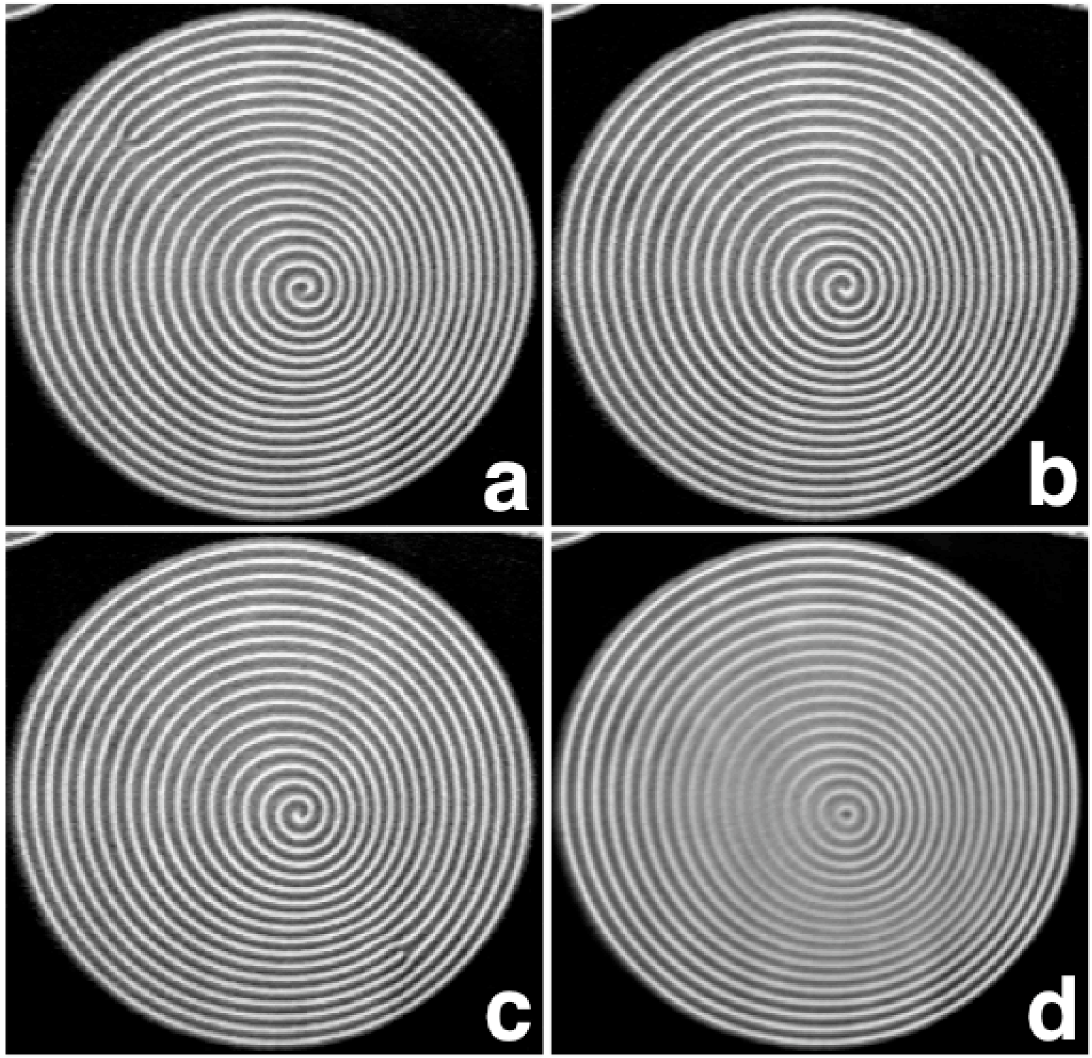

Figure 5.12: Off-center spiral in three orientations and the average. The time between (a) and (b) is 8.8 minutes (253 t_v); the time between (b) and (c) is 2.5 minutes (73 t_v). $\epsilon = 0.68$, $Pr = 1.38$.

Why? Where is the phase deformation?

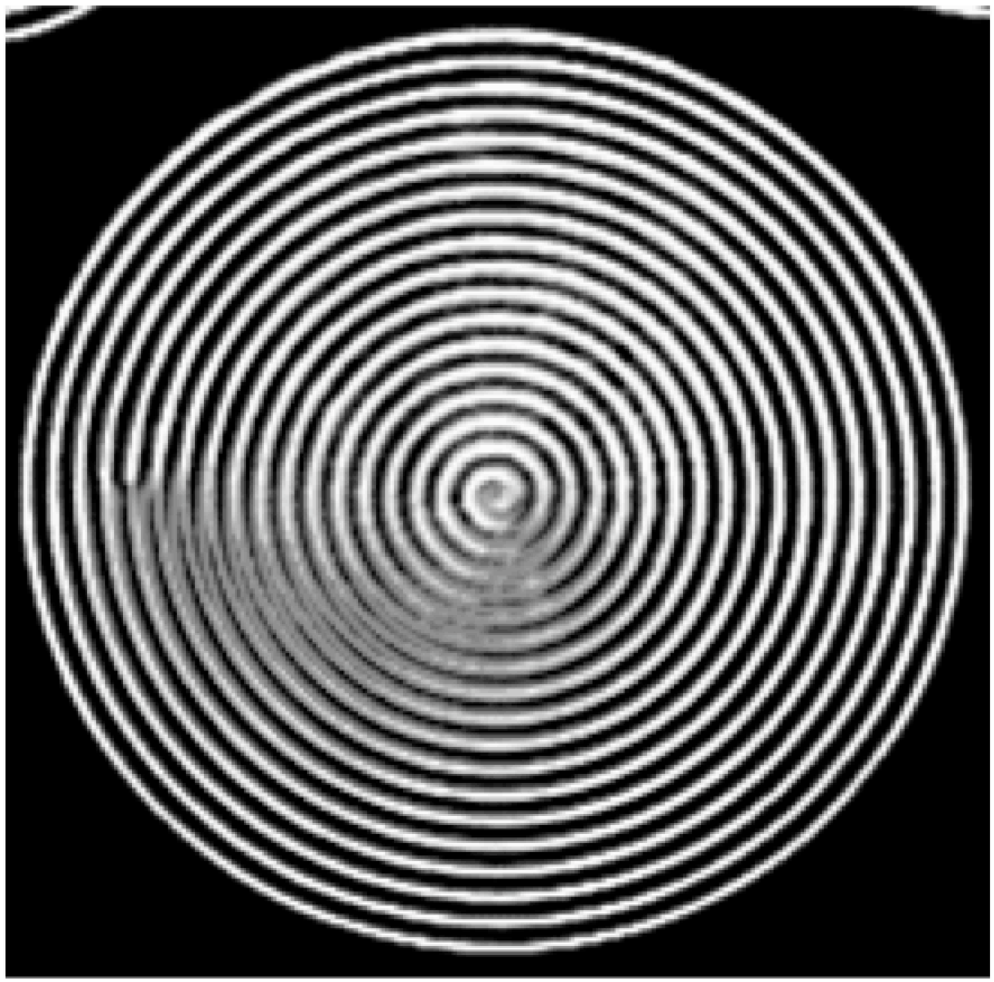

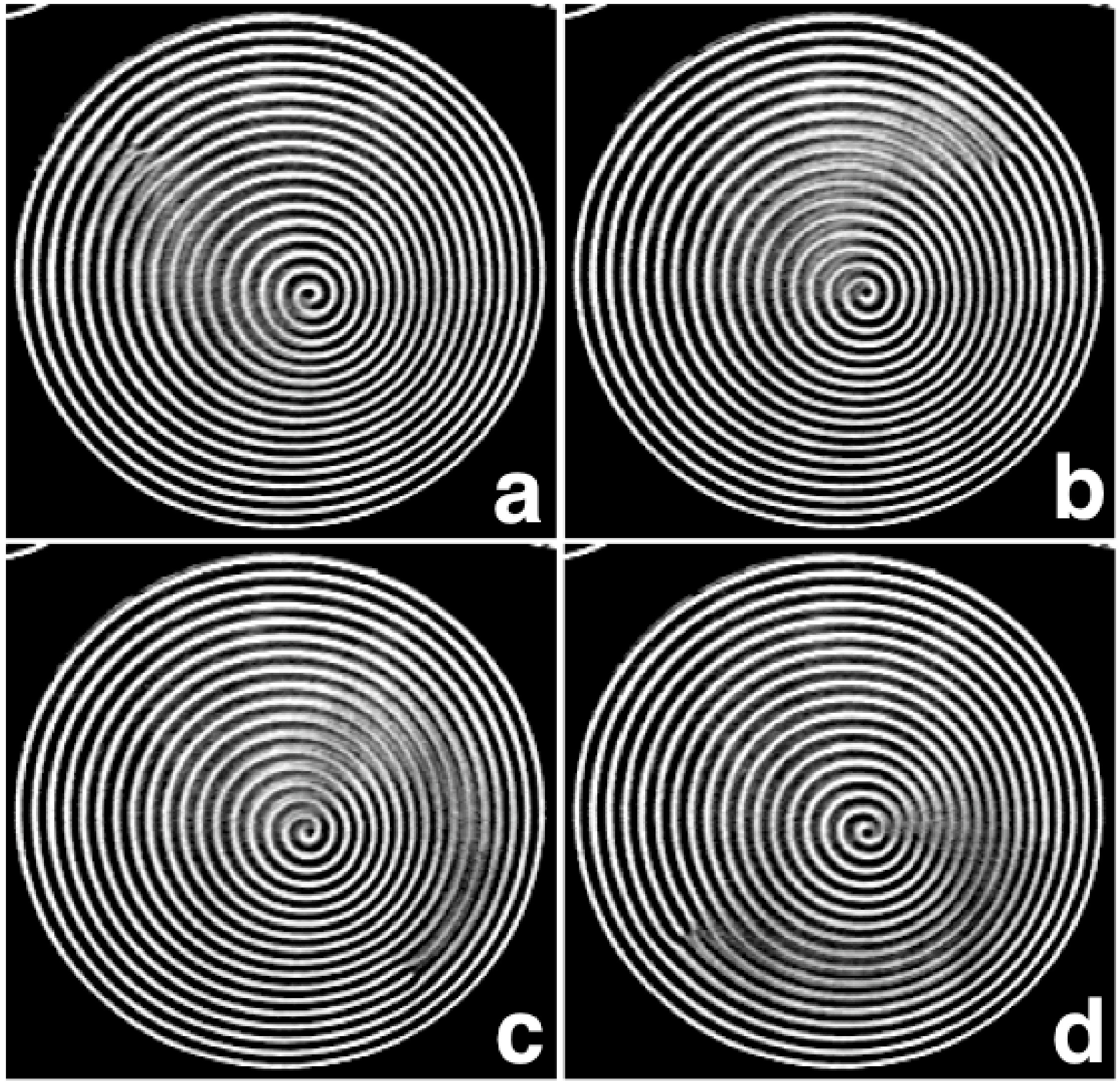

Figure 5.14: Average of off-center spiral (in four orientations) with the averaged spiral. The averaged spiral used is the same as figure 5.12d. The spiral used in frames (a), (b) and (c) correspond to the same frames in figure 5.12. The time between (a) and (b) is 8.8 minutes (253 t_v); the time between (b) and (c) is 2.5 minutes (73 t_v); the time between (c) and (d) is 3.2 minutes (93 t_v). $\epsilon = 0.68$, $Pr = 1.38$.

1-armed spiral wavenumber

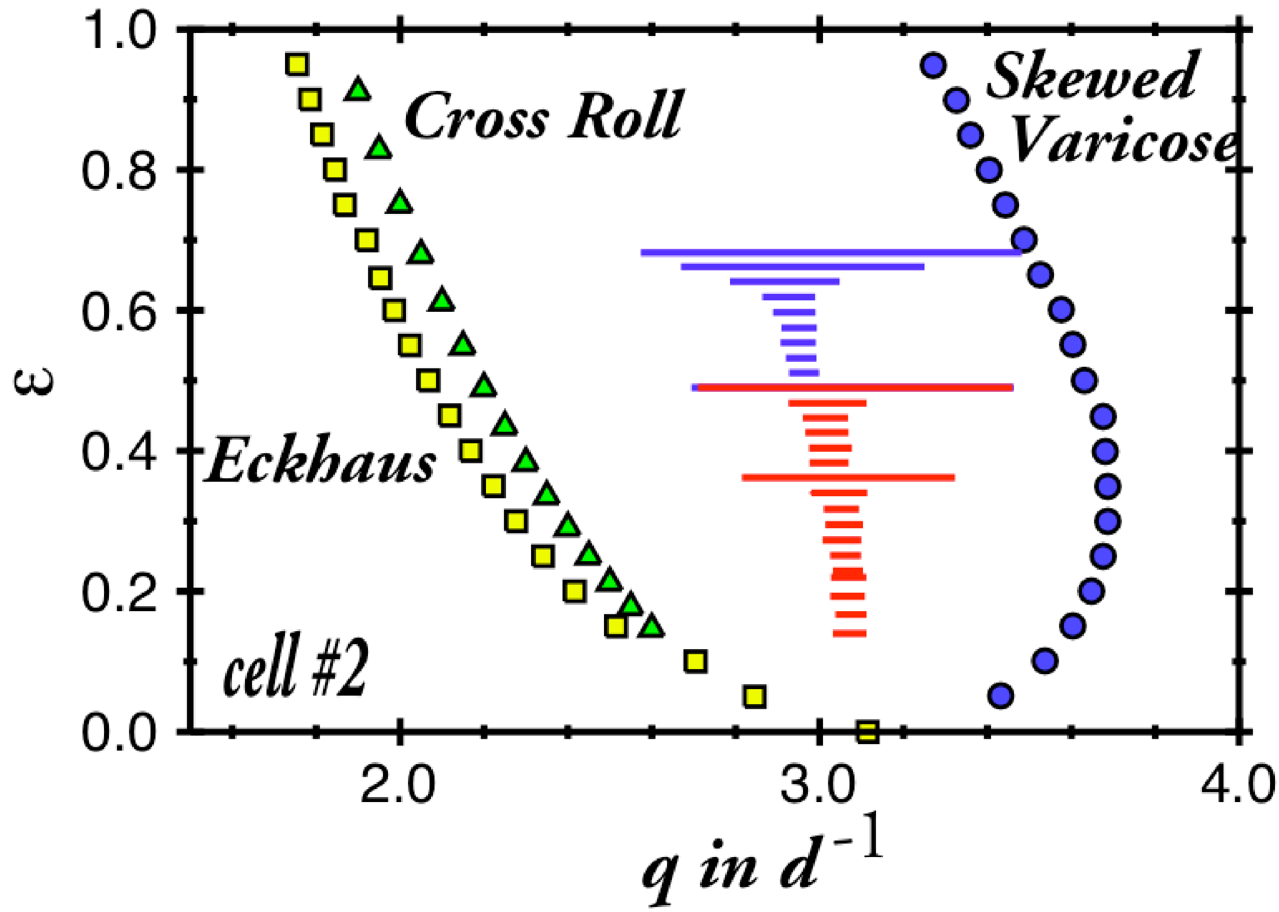

rotation period

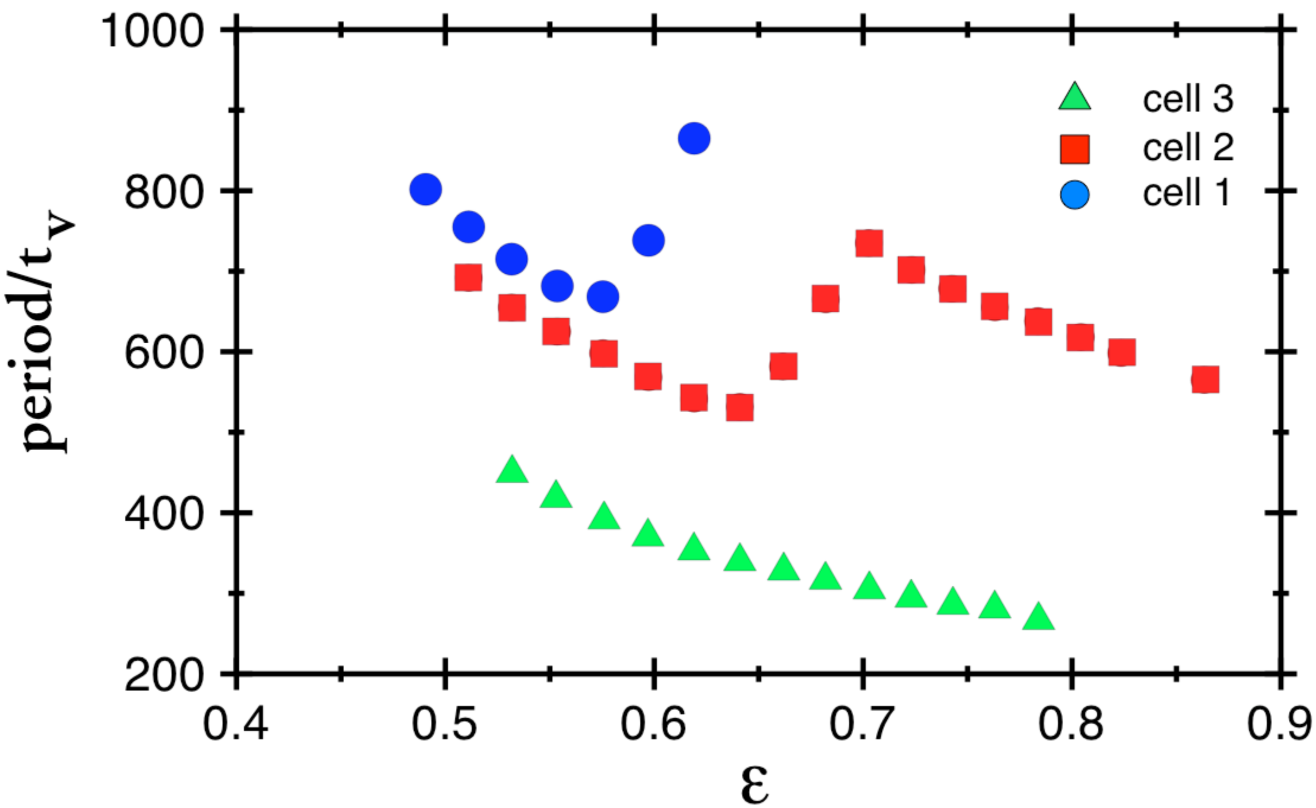

averaged tip velocity

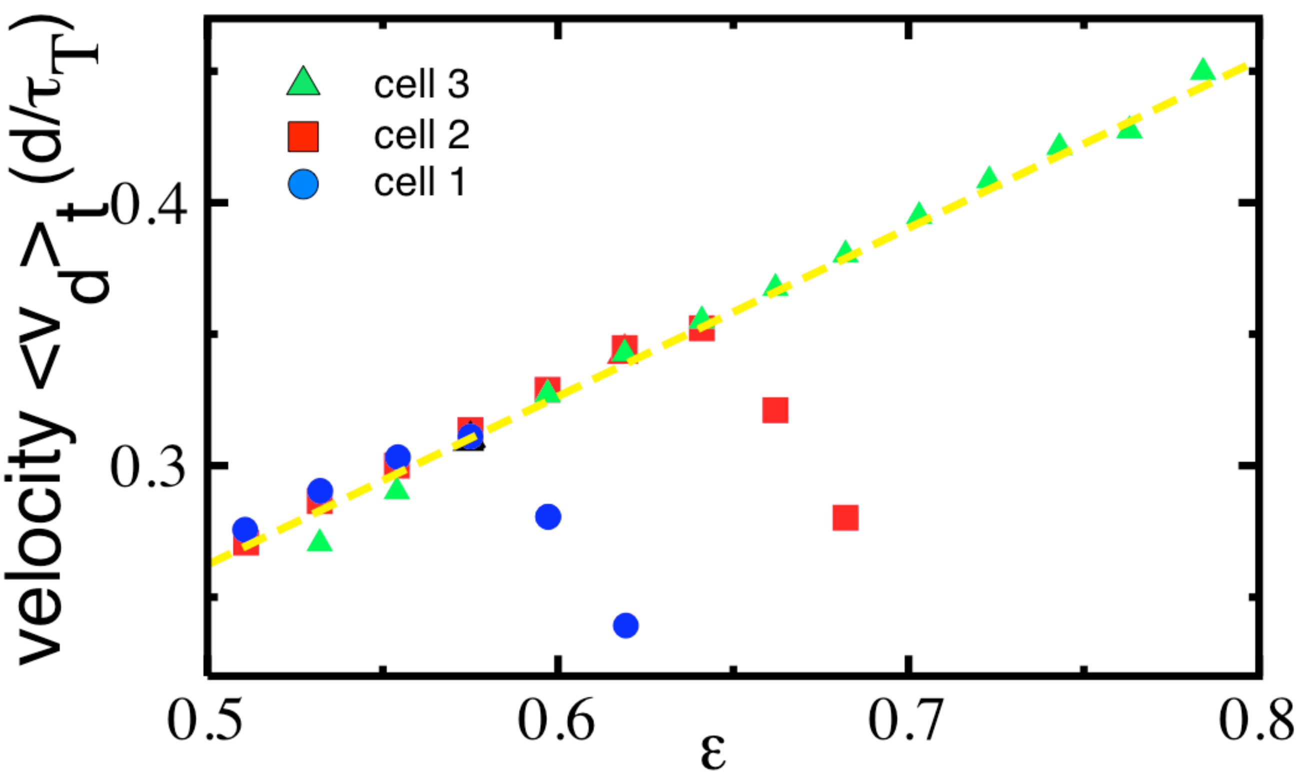

different from chemical spirals !

Results so far:

period of rotation prop. 1/r

time average of spiral gives underlying target

Question:

What determines the spiral rotation ?

Topological condition for rotation ?

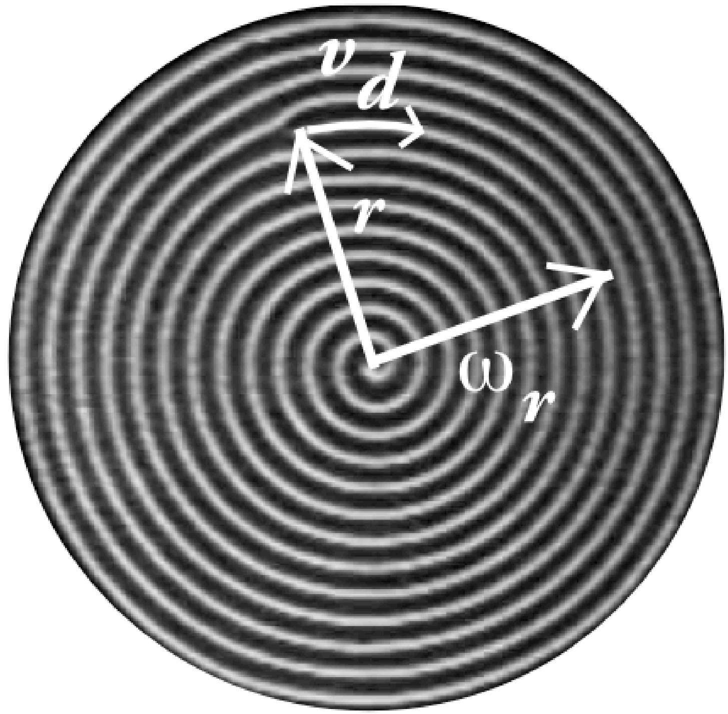

defect revolves with velocity v_d ***at radius*** r

==> ***frequency*** $\omega_d = v_d/r$

rolls travel outward with frequency ω_r

rigid rotation $\boxed{\omega_r = \omega_d = v_d/r}$

What do we know about v_d?

Tesauro and Cross, PRA 34 *(1986) 1363*

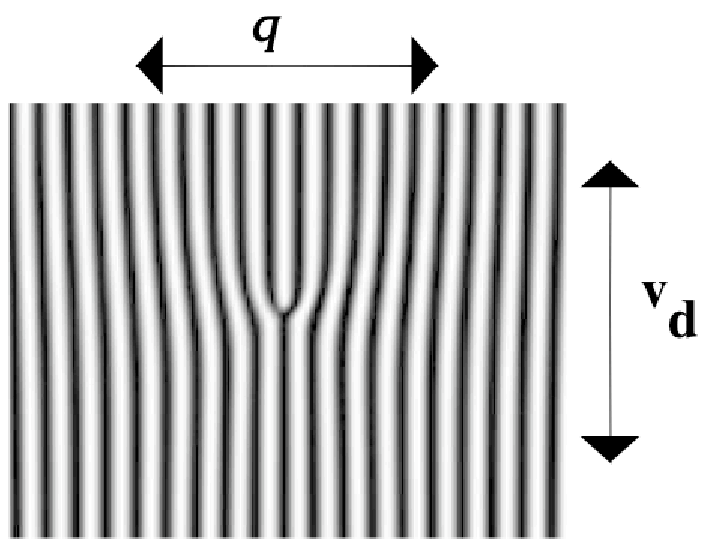

defect moves with v_d ***in background wavenumber*** q

$$\boxed{v_d = \beta\,(q - q_d)}$$

$$q = q_d \implies v_d = 0$$

"optimal" wavenumber q_d ***!***

Can we check this experimentally ?

Yes !

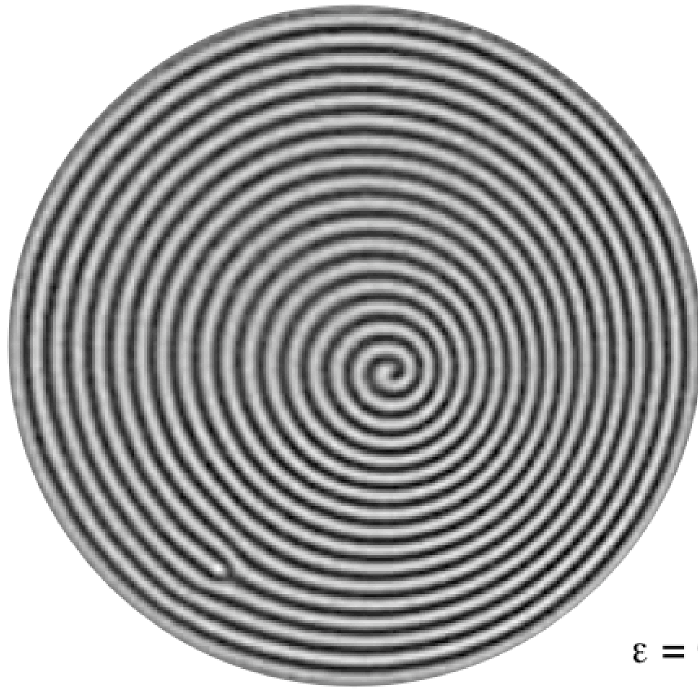

spirals move off center with increasing ε *!*

defect moves fast in compressed regions !

defect moves slow in dilated regions!

Defect Positions:

averaged

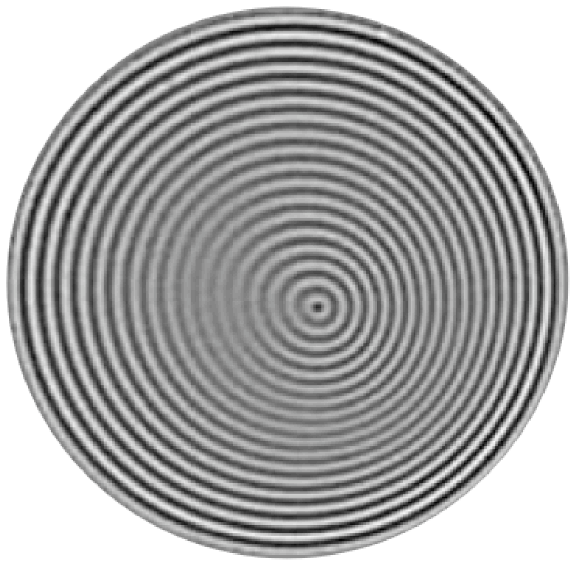

wavenumber

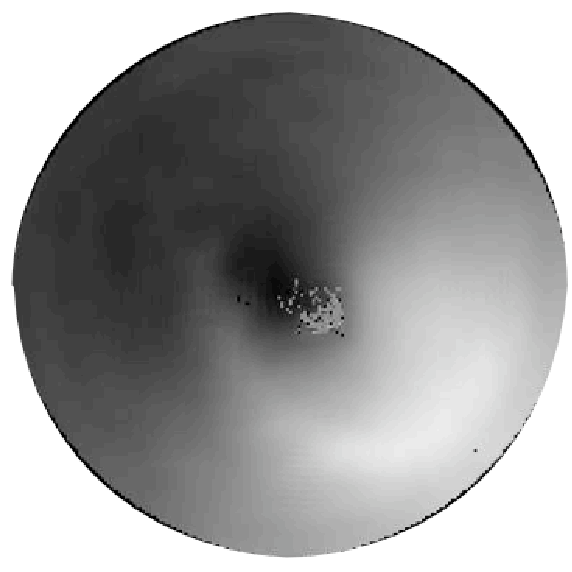

wavenumber

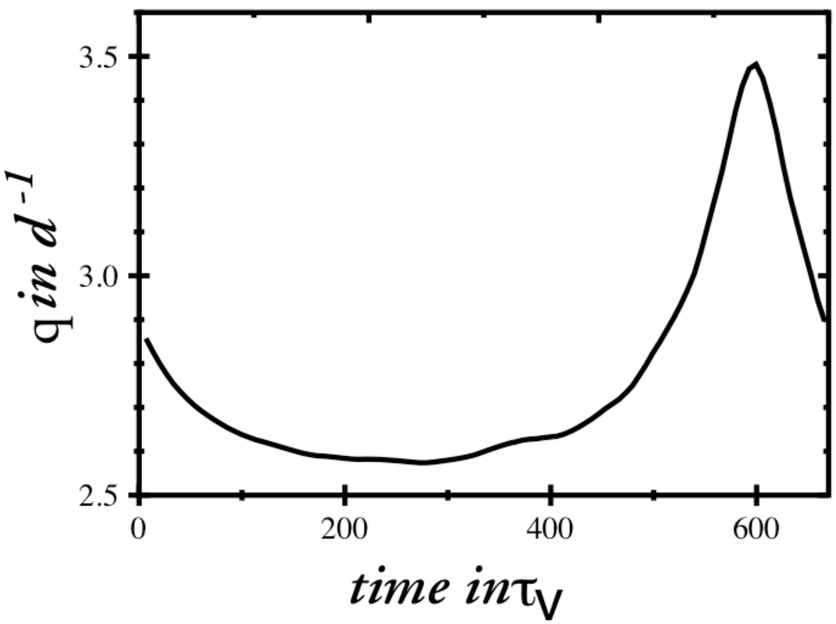

3.5
3.0
2.5
q *in d*$^{-1}$
0
200
400
600
time in τ_V

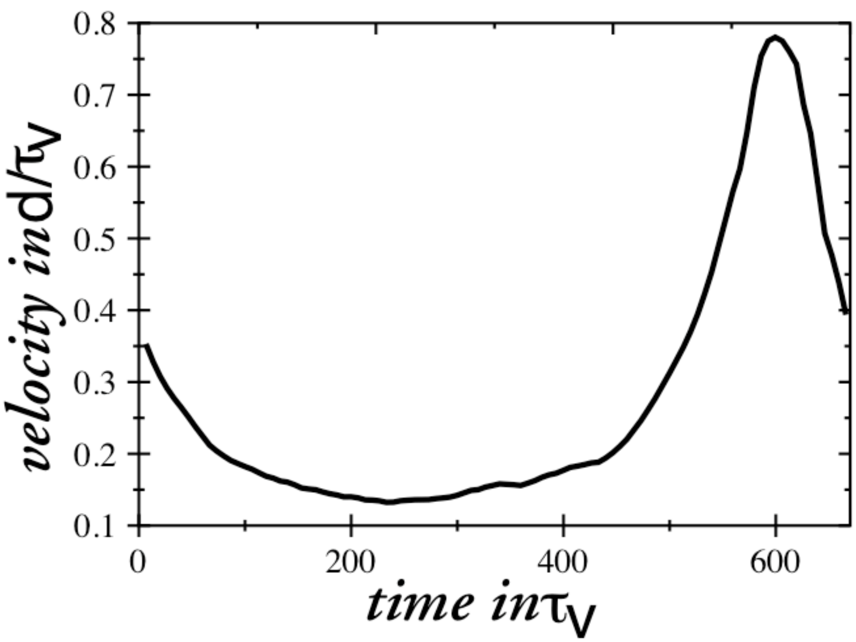

0.8
0.7
0.6
0.5
0.4
0.3
0.2
0.1
velocity in d/τ_V
0
200
400
600
time in τ_V

velocity vs. wavenumber

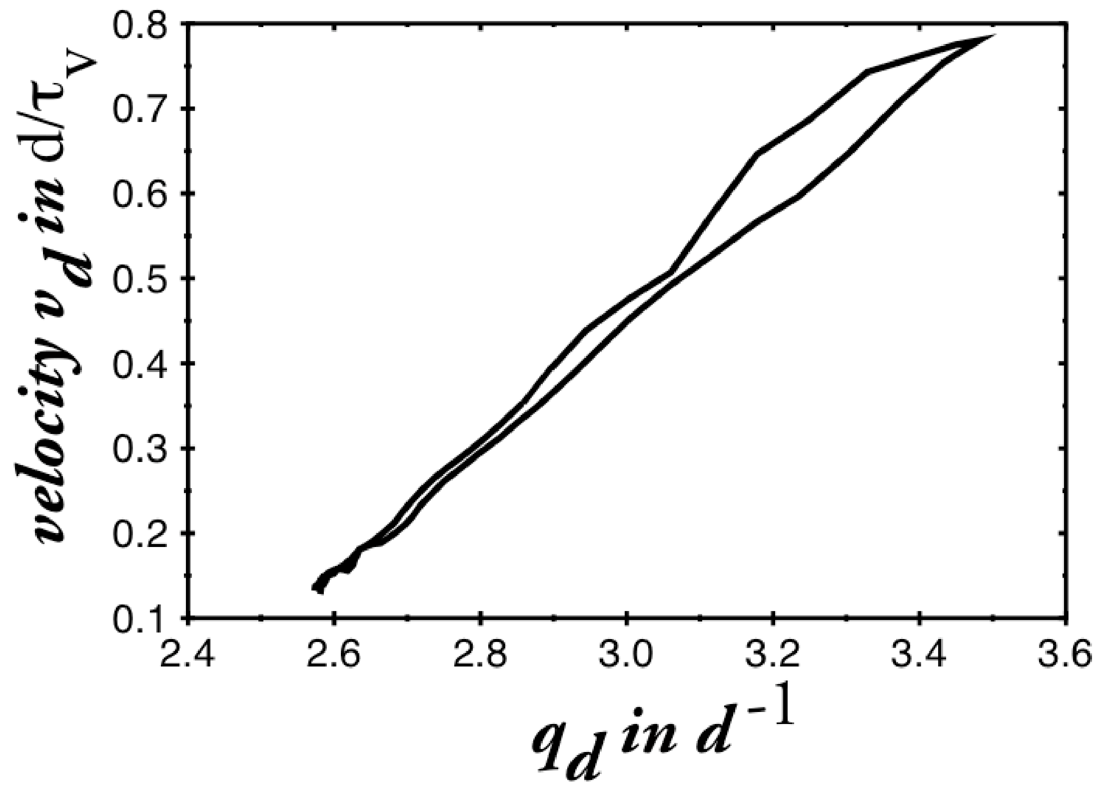

- excellent agreement with Tesauro-Cross

$$\boxed{v_d = \beta\,(q - q_d)}$$ ✓

- slight ε dependence !

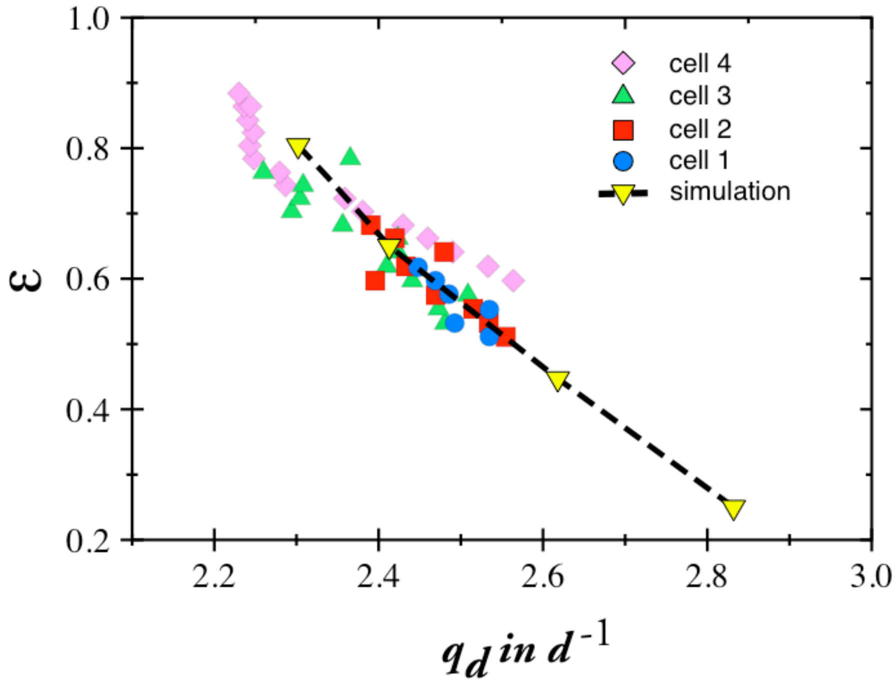

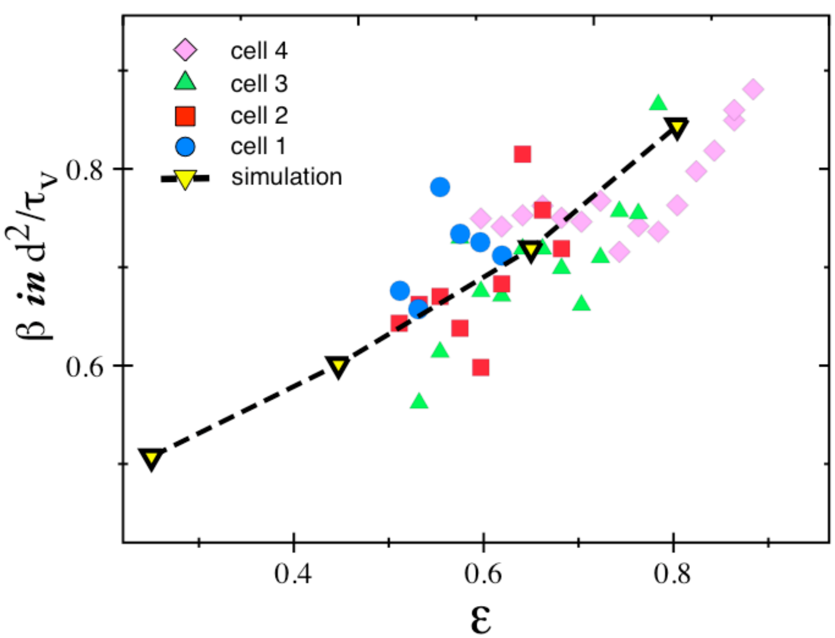

Spiral Rotation (part 2)

Cross and Tu , PRL 75 *(1995) 834*

Cross , Physica D **97** *(1996) 65*

Li, Xi and Gunton , PRE **54** *(1996) R3105*

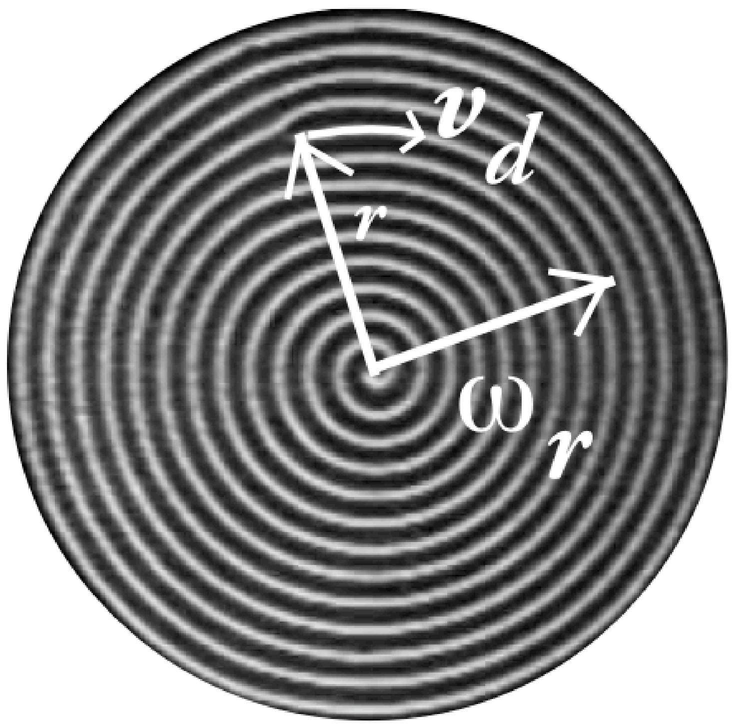

1-armed: $\omega_r = \omega_d = v_d/r$

m-armed: $\omega_r = m\,\omega_d = m\,v_d/ r$

phase equation: $\omega_r = \alpha\,(q_t - q)/r$

===> $\boxed{m\,v_d = \alpha\,(q_t - q)}$

"optimal" target wavenumber q_t ***!***

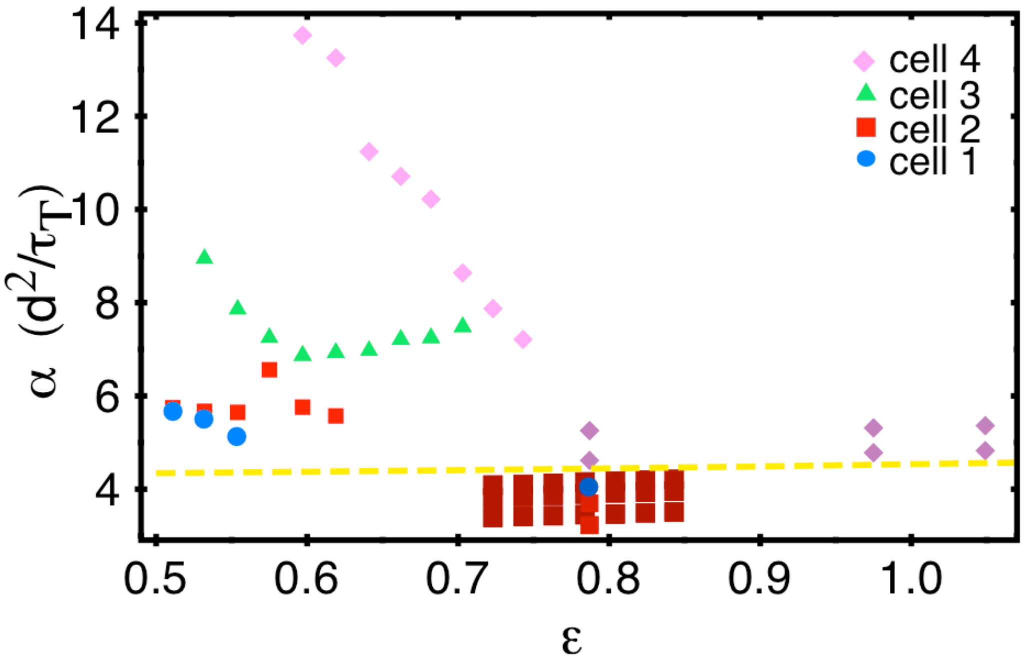

$$\alpha = 2D_{\|}(q_T) = -2\,\frac{\sigma(q_T)}{K^2}\bigg|_{K\to 0}$$

- excellent agreement with predictions from phase equation:

$$\boxed{m\, v_d = \alpha\,(q_t - q)}$$

- system size dependence !

Summary

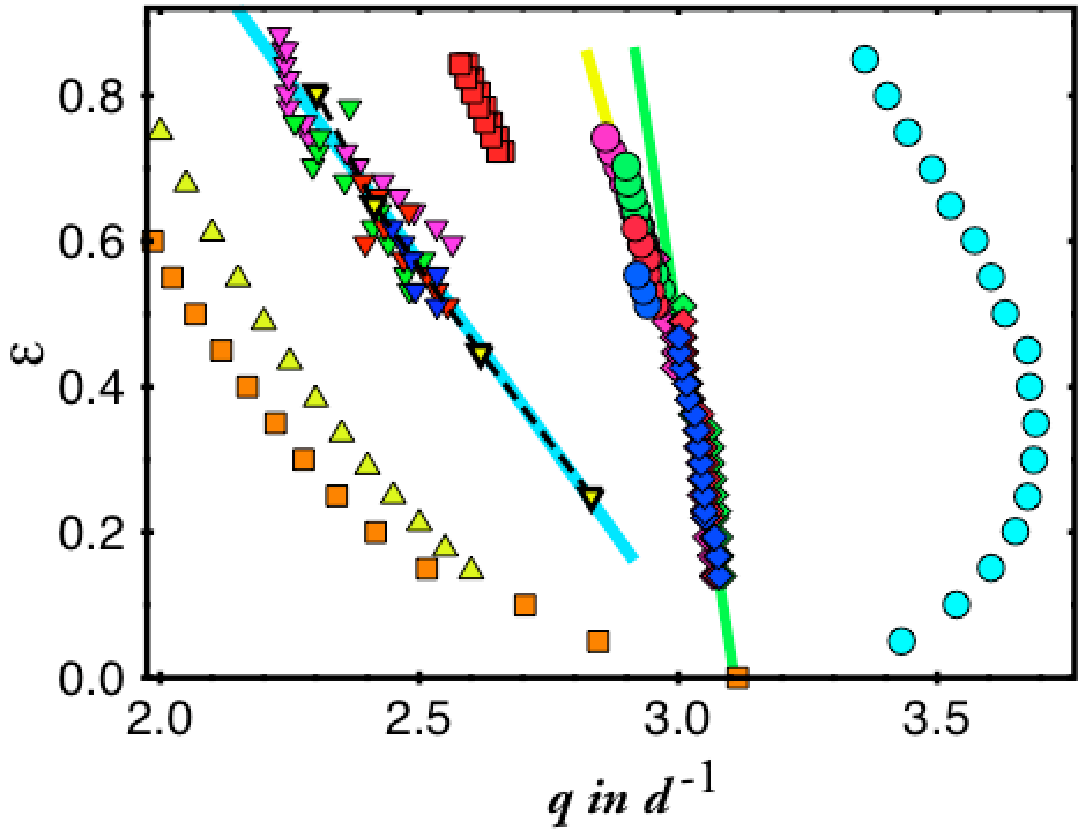

- *On-center Spirals :*
  Tip-defect moves to decrease wavenumber.
  Target travels outward to increase wavenumber.

- *Off-center Spirals:*
  Tip defect agrees well with phase equation prediction!

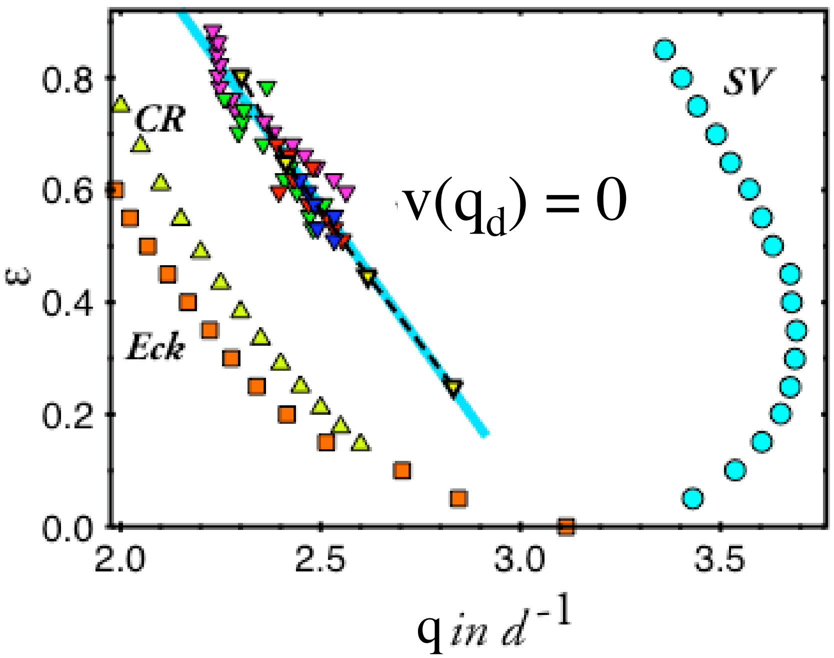

$$\boxed{\upsilon = \beta\,(q - q_d)}$$ ✓

What determines q_d?

Prandtl# dependence ?

Conjecture

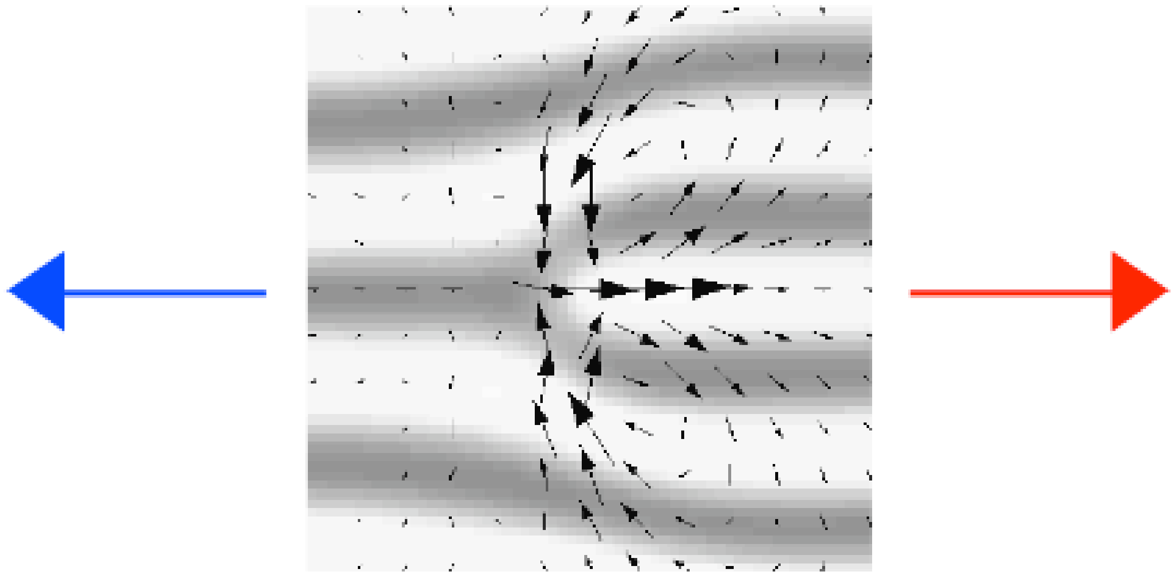

- meanflow advects roll pair out of system
  decreases wavenumber - Prandtl# dependent
- potential effects move roll pair into system
  increases wavenumber - Prandtl# independent

Generalized Swift-Hohenberg Equation

$$\frac{\partial}{\partial t}\Psi + (\vec{U}.\nabla)\Psi = [\varepsilon - (1-\nabla^2)^2]\Psi - \Psi^3$$

$$\vec{U} = (U_x, U_y) = (\frac{\partial}{\partial x}\xi, -\frac{\partial}{\partial y}\xi)$$

$$(\frac{\partial}{\partial t} - \Delta + 2)\Delta\xi = g(\nabla(\Delta\Psi)) \mathrm{x} \nabla\Psi)\hat{e}_z$$

- can be derived from a potential $\frac{\partial}{\partial t}\Psi = -\frac{\delta V}{\delta \Psi}$
- roll curvature generates meanflow $g \sim Pr^{-1}$
  non-potential effect

- ***temperature field ψ independent of g***

$g = (2.5, 5, 7.5, 10, 15, 20)$

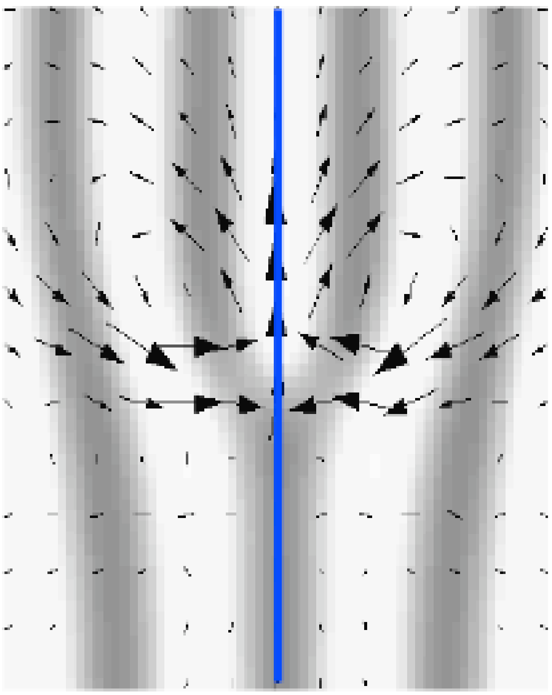

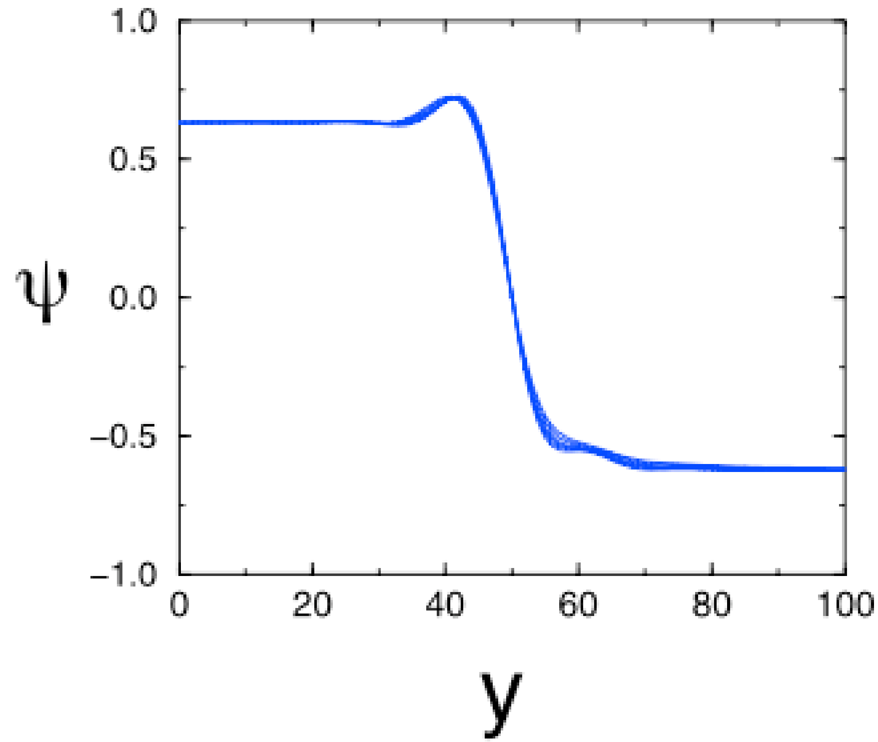

GSH-simulations 512 x 256 (1024 x 512)

$\varepsilon = 0.3$, $q = 0.95$

● *normalized meanflow* U_y/g *field independent of g*

$g = (2.5, 5, 7.5, 10, 15, 20)$

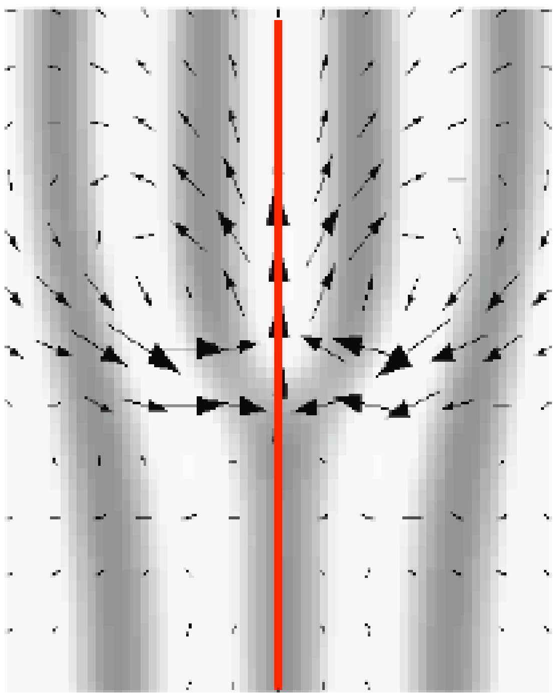

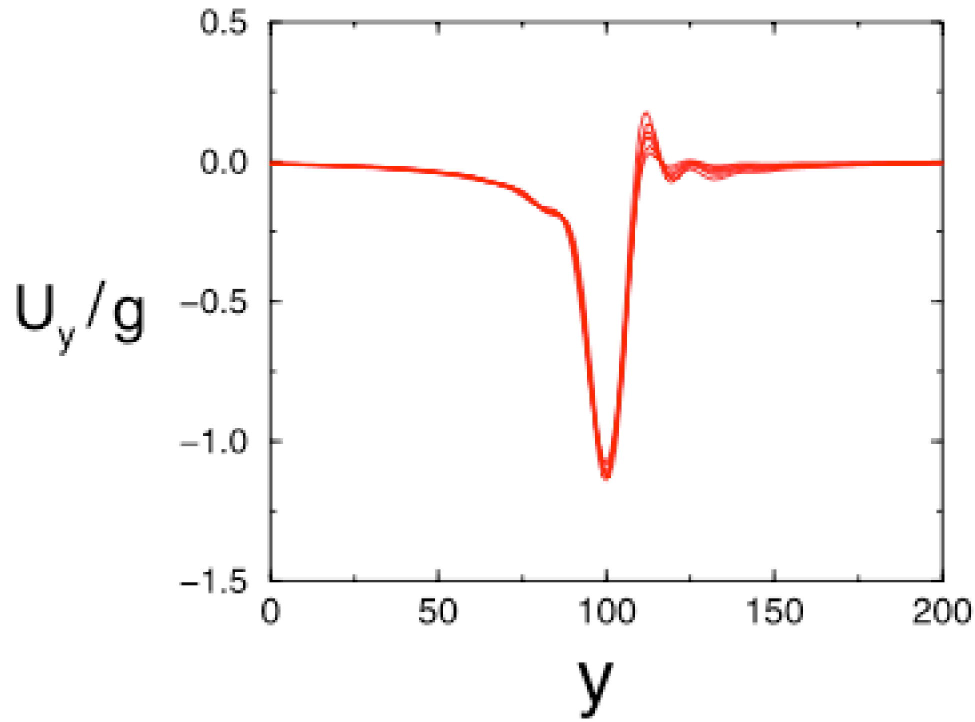

GSH-simulations 512 x 256 (1024 x 512)

$\varepsilon = 0.3$, $q = 0.95$

comoving coordinate system:

$$-v\frac{\partial\Psi}{\partial y} = [\varepsilon - (1-\nabla^2)^2]\Psi - \Psi^3 - U_y\frac{\partial\Psi}{\partial y}$$

with $U_y(0,y) \approx g f(y)$

$$0 \approx \int dy\,([\varepsilon - (1-\nabla^2)^2]\Psi - \Psi^3) - g\int dy f(y)\frac{\partial\Psi}{\partial y} + v\int dy\frac{\partial\Psi}{\partial y}$$

===> $0 \approx c_1 - g c_2 + v c_3$ ===>

$$v \approx -\frac{c_1}{c_3} + \frac{c_2}{c_3}g$$

with $\langle U_y\rangle = \int dy f(y)\, g = c' g$

$$v(\bar{q}) \approx v(\bar{q}, g{=}0) + \frac{c(\bar{q})}{c'}\langle U_y\rangle$$

Numerical test:

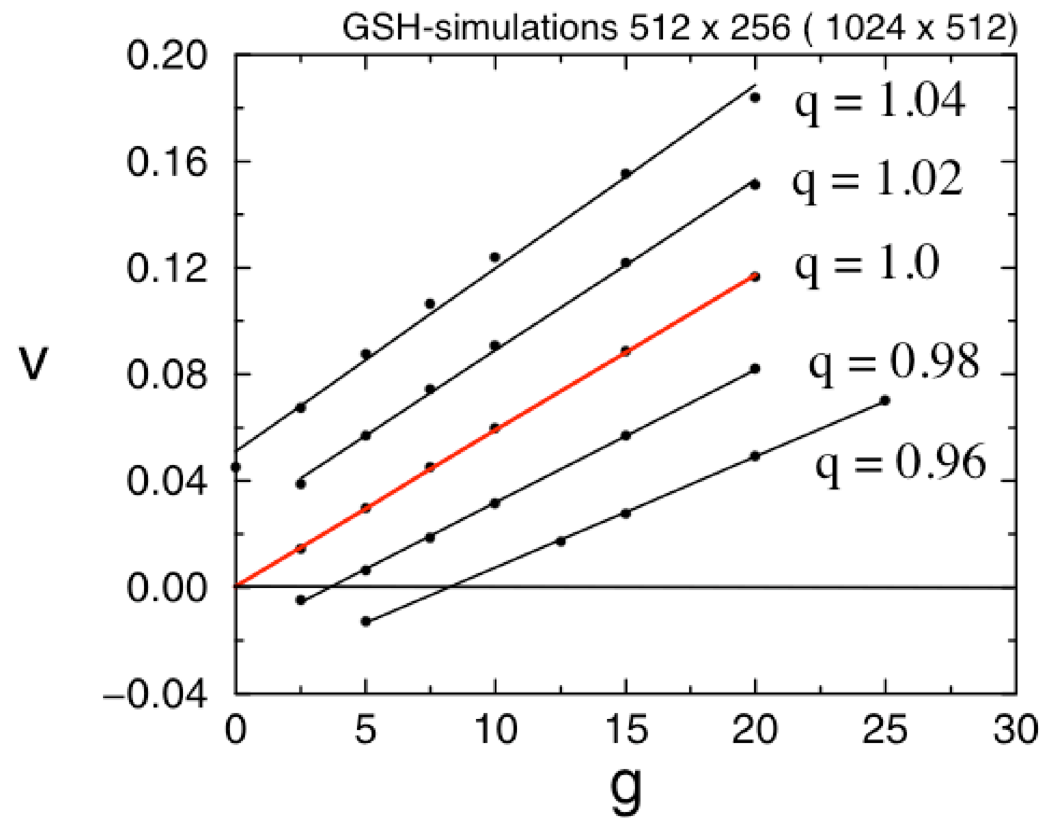

Rayleigh-Bénard Convection

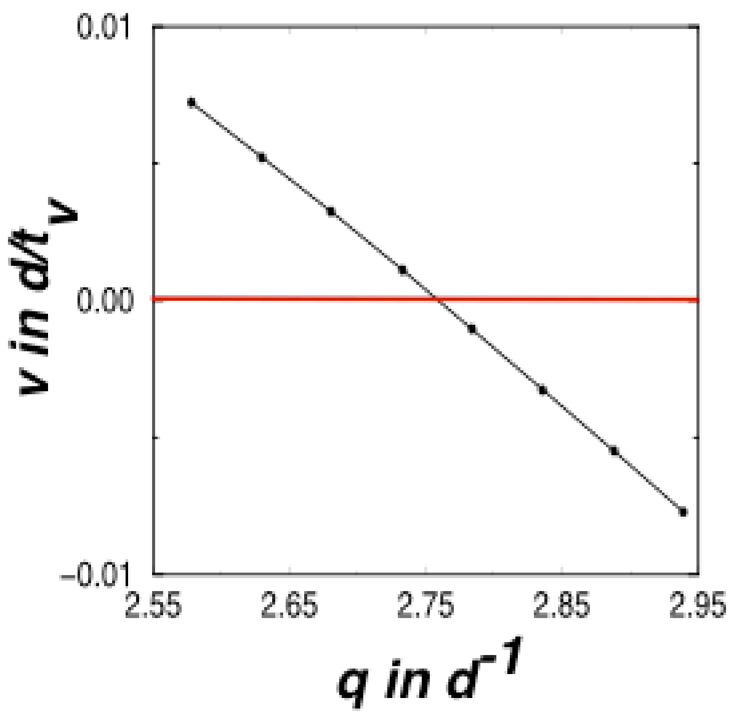

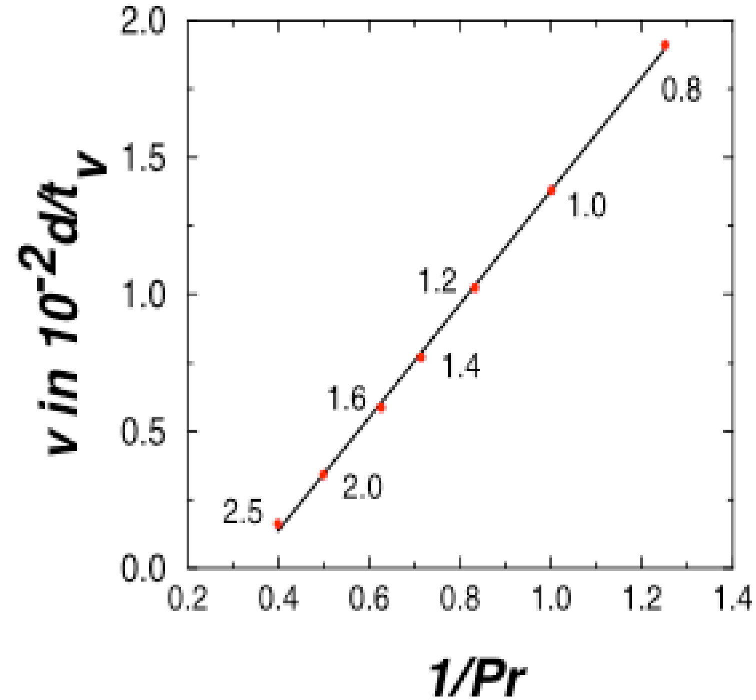

$$v(\bar{q}, Pr) = v(\bar{q}, \infty) + c(\bar{q}) \frac{1}{Pr}$$

Bound Dislocations:

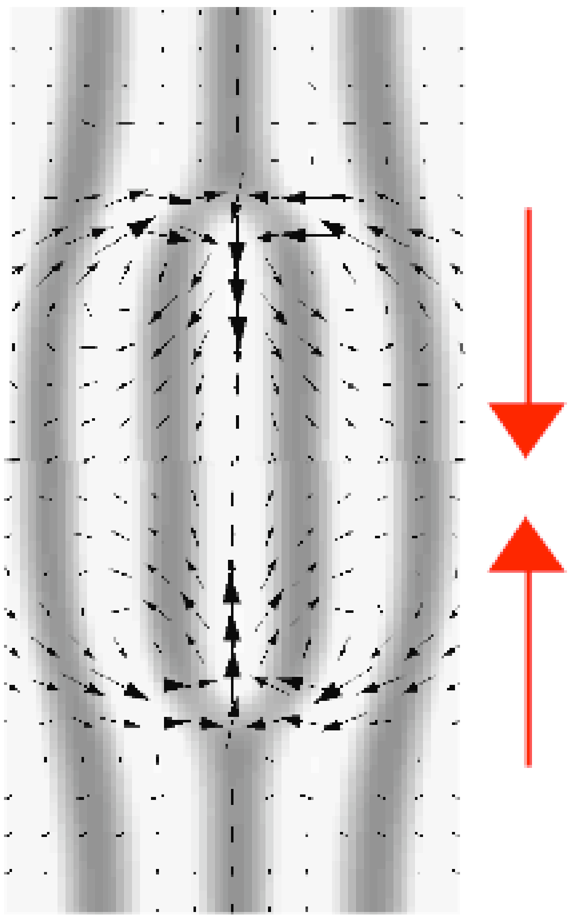

meanflows superimpose

$\Downarrow$

effective meanflow decreases

$\Downarrow$

bound pair

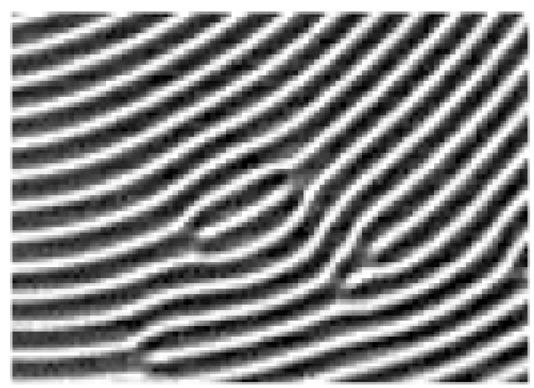

RBC experiment

(E.B., J. deBruyn, G. Ahlers, D. Cannell 1992)

Summary

- *Potential ($Pr = \infty$) moves dislocation towards bandcenter.*
- *Meanflow advects dislocation as to decrease* q

$$\boxed{v(q,\mathrm{Pr}) = v(q,\infty) + c(q)\frac{1}{\mathrm{Pr}}}$$

- *Dislocation stationary for "meanflow = potential ".*
- *Bound dislocation due to meanflow interaction.*

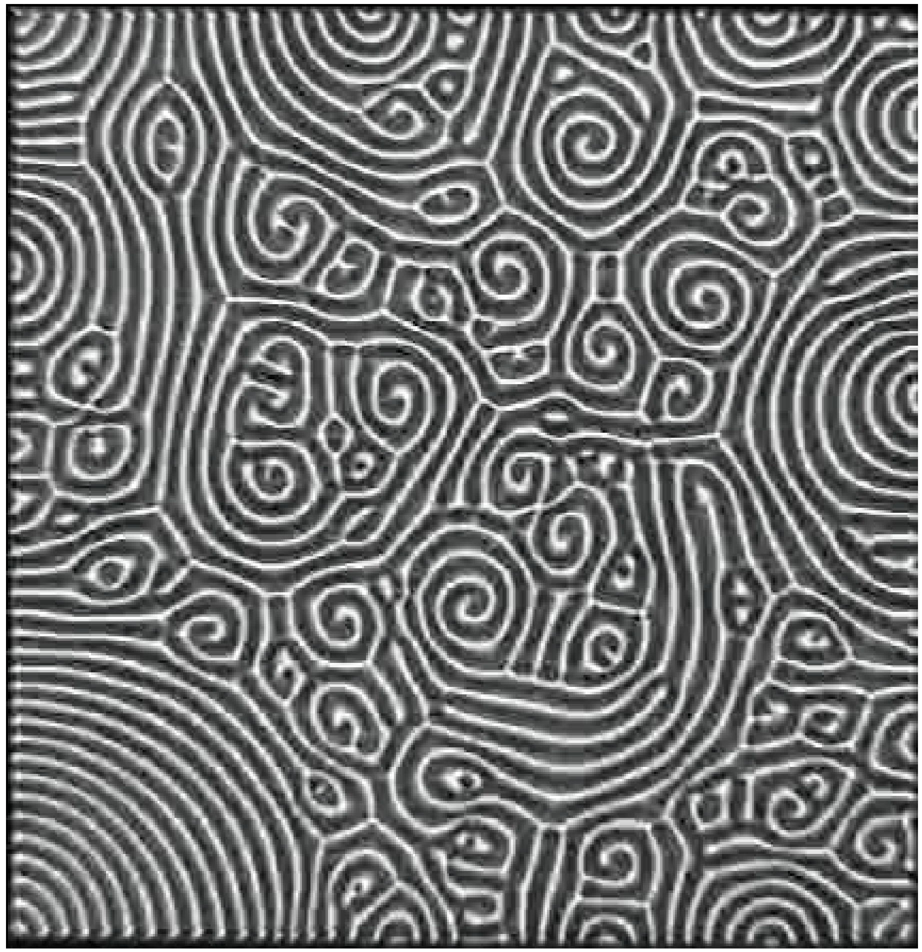

Spiral Defect Chaos (Morris et al. 1992)

The End